

Avalanches and deformation in glasses and disordered systems

Contribution to the book *Spin Glass Theory and Far Beyond - Replica Symmetry Breaking after 40 Years*

Alberto Rosso

Université Paris Saclay, CNRS,LPTMS, 91405, Orsay, France

James P. Sethna

LASSP, Cornell University, Ithaca, NY 14853, USA

Matthieu Wyart

*Institute of Physics, École Polytechnique Fédérale de
Lausanne (EPFL), CH-1015 Lausanne, Switzerland*

In this chapter, we discuss avalanches in glasses and disordered systems, and the macroscopic dynamical behavior that they mediate. We briefly review three classes of systems where avalanches are observed: depinning transition of disordered interfaces, yielding of amorphous materials, and the jamming transition. Without extensive formalism, we discuss results gleaned from theoretical approaches – mean-field theory, scaling and exponent relations, the renormalization group, and a few results from replica theory. We focus both on the remarkably sophisticated physics of avalanches and on relatively new approaches to the macroscopic flow behavior exhibited past the depinning/yielding transition.

I. INTRODUCTION

Rigid systems, put under stress, will often respond through a series of avalanches [1–3] with a broad distribution of sizes and durations.¹ Faults in the Earth exhibit earthquakes spanning many decades of size [5–8] when stressed by the motion of tectonic plates. Iron placed in a growing magnetic field will emit Barkhausen crackling noise (both acoustic and electromagnetic) as the internal magnetic domain walls shift between metastable states [9,

¹ Warning: Everyday avalanches in sandpiles, or of snow or rocks on mountains, rarely exhibit the fractal, scale invariant behavior we study here [4].

10]. Raindrops on your windshield advance in bursts – their leading edges, pinned by dirt, releasing as they grow and merge [11]. Avalanches also arise microscopically in systems that usually are viewed as responding smoothly to an external stress. Your fork, bending irreversibly when you try to cut through a tough piece of meat, responds through many dislocation avalanches with a distribution of sizes – measurable, for example, in experiments where nanopillars of metal are compressed [12–17]. Toothpaste squeezed out of a tube yields above a critical stress through a jerky set of avalanches.

In all these systems an avalanche starts from a weak spot that becomes unstable and slips. This triggers other instabilities nearby that in turn infect other regions – sometimes halting quickly, and sometimes sweeping over vast regions before halting. Some systems exhibit avalanches of all scales (sometimes termed ‘crackling noise’) only when delicately tuned to balance between stability (only local events) and instability (continuous flow). We shall see that many systems can either *self-organize* to this balancing point, or exhibit *generic scale invariance* – with events of all scales due to long-range non-monotonic (i.e. of varying sign) interactions.

These avalanches are characteristic of systems that have a complex energy landscape (well studied in other chapters of this book). Increasing the stress on the system ‘tilts’ this landscape, and the avalanches represent transitions from one metastable valley to another. For a sufficiently large tilt, rigidity can be lost and the system flows continuously. We focus on unifying concepts that describe both the avalanche-type response and continuous flows when it occurs, in systems ranging from disordered magnets and granular materials to epidemics, raindrops, and brain activity. We shall explain, without extensive formalism, how *scaling* and *renormalization-group* methods unify all of these systems, and elucidate the important physics that make these systems different from one another.

Our contribution is organized as follows. In section II, we introduce a few of the many systems exhibiting collective avalanches and crackling noise: epidemics, depinning of lines and interfaces in random media, yielding in amorphous solids such as glasses and foams, and dense granular flows. In the first two cases, system-spanning avalanches occur at a critical point, while in other cases they occur in an entire phase. In section III, we explain these facts by introducing the notion of *excitations*, as regions of the material that are about to undergo an instability. If sufficiently long-range interactions are present, requiring stability of the material constrains the density of excitations, which in turn implies a generic scale

invariance in the entire rigid phase. In sections IV, V and VI we introduce renormalization group results and scaling arguments. They apply but differ in the systems considered, allowing one to both compare these systems and build a detailed understanding of several phenomena, including the shape of avalanches or their connection with stationary flows when rigidity is lost. In section VII, we conclude by emphasizing key open questions of this field.

II. SYSTEMS CONSIDERED

Avalanches appear in many areas, both in science and engineering and in other fields. In addition to the examples above, avalanche models have been used to describe fracture precursors in quasi-brittle material like bones and seashells [18], bubble avalanches in foams [19], fluids invading porous media [20, 21] (like milk invading puffed rice cereal [22] or coffee soaking into a napkin [23]), vortex avalanches in superconductors [[3], Ch. 9] and neutron stars [24], wars [25], neural avalanches in brain tissue [26, 27], noise while tearing paper [28] and while crumpling paper or candy wrappers [29, 30], and clapping after concert performances [31]. In this section, we introduce four phenomena we focus on: the mean field theory of epidemics, the depinning transition of an elastic manifold in a disordered environment, the plasticity of simple yield stress materials, and the jamming transition in granular systems.

A. Mean-field pandemic model

Outbreaks of disease are a public-health manifestation of avalanche behavior. An unlucky person is infected by a bird, pig, or bat, and infects one or more surrounding people. Let R_0 denote the number of infections triggered by each formerly infected person; $R_0 \sim 12\text{--}18$ for measles, $2\text{--}3$ for influenza. For a new disease where nobody is immune, $R_0 < 1$ means that the disease will gradually disappear, $R_0 > 1$ implies that – if not stamped out early – it will cause a global pandemic. Near $R_0 = 1$, there is a phase transition, with avalanches (outbreaks that halt) on all scales for $R_0 \lesssim 1$.

This model is called the Bienaymé-Galton-Watson process [32, 33]. It is a *mean-field* model for avalanches, because there is no notion of space: everyone can infect anyone. It also describes a fully connected Ising model in a disordered material [34], where a spin flips

when its external field increases beyond its random threshold, increasing the external ‘mean field’ on all the other N spins enough to on average flip R_0 neighbors. In some cases, this mean-field aspect is not a realistic assumption: plants do not move, so crop diseases that spread locally have avalanches that are correlated in space.

Consider the number I_{N_R} of infected people at the time when N_R people have stopped being infectious (either recovered or deceased). Each person, before they recover, infects ξ_{N_R} others, where ξ is a random integer chosen from a Poisson distribution of mean $R_0 I_{N_R}$. For simplicity, we assume these infections happen at the time when the person recovers, implying $I_{N_R+1} = I_{N_R} + \xi_{N_R}$. This random walk halts at pandemic size S when I_S first touches zero; its size S is the number of random steps for the first return to the origin. The probability of a pandemic of size S at $R_0 = 1$ thus coincides with the probability that a random walk starting at the origin will have its first return after S steps, which can be calculated to be a power law $P(S) \sim S^{-\tau}$ with $\tau = 3/2$. Let us measure the distance to the critical point as $r = (R_0 - R)/R$. For $r \lesssim 0$ below threshold, the random walk starts positive ($I_1 = 1$) but has a negative drift – it is a biased random walk. For small avalanches near R_c , the accumulated drift $\Delta I = rS$ is negligible compared to the typical random walk distance $I_{\max} \sim S^{1/2}$, but for large avalanches the drift dominates, making large avalanches unusual. Equating the two, we expect the probability distribution of avalanches $P(S, r)$ is cut off at a size $S_{\max} \sim r^{-1/\sigma}$ with $\sigma = 1/2$. More precisely, $P(S, r)$ can be shown to follow

$$P(S, r) \sim S^{-3/2} \exp(-Sr^2/2) \sim S^{-\tau} \mathcal{P}(S^\sigma r) \quad \text{with } \mathcal{P}(X) = \exp(-X^2/2). \quad (1)$$

Here τ and σ are universal critical exponents, and \mathcal{P} is a universal scaling function of the invariant scaling ratio $X = S^\sigma r$. Universality signifies that changing our epidemic model to a more realistic stochastic SIR model (a ‘compartmental’ model discussing the susceptible, infected, and recovered populations), or a model with superspreaders, does not change the values for τ , σ , and \mathcal{P} that describe large epidemics. However, some features like cities can change the behavior away from mean-field in qualitative ways.

Scaling functions arise [35] whenever more than two parameters and properties are involved (here, probability P , depending on size S , and distance r to the critical point). Other examples include avalanche duration versus time as a function of r , scaling depending on the system size L , crossover scaling [9, 36], singular corrections to scaling, etc. We shall study a universal scaling function for the average temporal shape of avalanches, which has

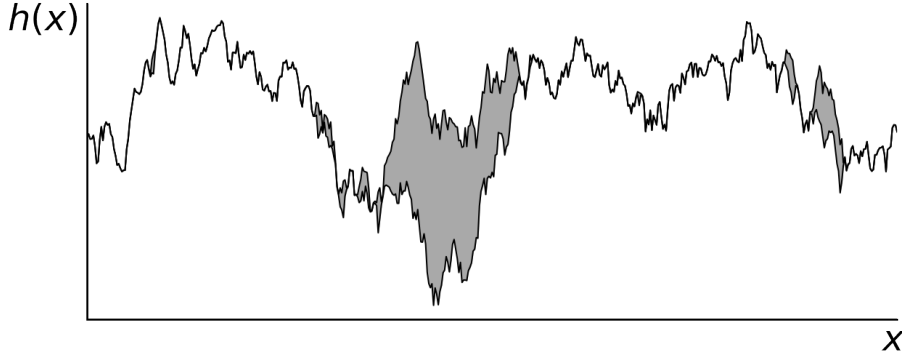


FIG. 1. **Depinning** of a one-dimensional manifold in a two dimensional environment. An increasing external field causes the manifold to locally destabilize, moving from one configuration to another in an avalanche (large gray region, of area S). If there are long-range forces in the problem, this event may cause other distant segments to destabilize as well (small gray regions to right).

two properties depending on two parameters, in section IV C.

Finally, note that to obtain avalanches of all scales requires to tune a parameter like R_0 to a critical point. However, in various cases this parameter can spontaneously evolve to that value, a phenomenon called *self organized criticality* [37]. In our disease outbreak model, imagine we add a term which describes the societal response to widespread illness – wearing masks, getting immunized, avoiding large gatherings. As outbreaks become large and alarming, these responses will tend to reduce the effective interactions, tuning R_0 down until just below the threshold for a pandemic [38].

B. Depinning transitions

View Fig. 1 as a one-dimensional elastic interface, pushed through a disorder environment by applying a force per unit length f . Examples of this situation abound¹: it could represent a magnetic film, magnetized ‘up’ below the jagged interface, and ‘down’ above the interface with a forcing that depends on the applied magnetic field [10]; or the triple line formed at the edge of a drop on your windshield, forced by gravity [11]. These phenomena are well described as the propagation of a single-valued front $u(r, t)$, where r and u are the horizontal and vertical coordinates of the interface. Neglecting inertial effects, the equation

¹ One can also view it as a two-dimensional disordered crystal with a jagged dislocation line pinned on impurities, or a polymer pinned on a disordered surface, or an oil-water interface in porous rock [20].

of motion of our front might be modeled as a disordered partial differential equation of this class [39, 40]:

$$\partial_t u(r, t) = f_{\text{el}}[u] + f_{\text{dis}}[u(r, t), x] + f. \quad (2)$$

Here f_{el} is the elastic force trying to restore the straight interface, f_{dis} is the force due to the random potential, and f is the external drive. The solution of this class of equations shows a continuous phase transition with the velocity playing the role of the order parameter and the force acting as the control parameter [41–45]. In particular, below a critical *depinning* force f_c the steady velocity is zero.

Avalanches: If we increase that external field for $f < f_c$, we can destabilize a weakly-pinned region, triggering an avalanche (see Fig. 1). Just as in the epidemic model, below f_c these avalanches have a size distribution $P(S, f) \sim S^{-\tau} \mathcal{P}(S(f_c - f)^{1/\sigma})$, becoming scale free when the force approaches $f = f_c$. Individual avalanches smaller than the cutoff $S_{\text{max}} = (f_c - f)^{1/\sigma}$ will spread over a spatial extent $\sim S^{1/d_f}$, where $d_f = 1/(\sigma\nu)$. They will have a duration in time $\sim S^{z/d_f}$ that goes as their spatial extent to the power z . Avalanche distributions have been extensively studied in the literature [46–52].

Flow properties are singular: For $f > f_c$, the interface will begin moving with a mean velocity $v \sim (f - f_c)^\beta$ in a jerky fashion, with correlated jumps that mimic the avalanches found just below f_c . Similarly to equilibrium continuous phase transitions, the collective nature of this intermittent dynamics arises from the existence of a correlation length $\xi \sim |f - f_c|^{-\nu}$ that diverges when the force approaches f_c .

Fractal structure: At the depinning threshold, the interface is fractal, with a roughness that is characterized by a typical vertical height change $u(r, t) - u(r', t) \sim (r - r')^\zeta$ corresponding to a height-height correlation function $C(r) = \langle (u(r') - u(r' + r))^2 \rangle \sim r^{2\zeta}$.

The elastic force f_{el} on a domain wall can involve long-range interactions [53]. This is the case for the triple line of a raindrop on glass [11, 54] (and also of crack fronts propagating in brittle materials [55, 56]). The elastic force on the droplet interface must include the surface tension energy of the wiggly drop shape imposed by the jagged air-water interface $u(r)$, hence $f_{\text{el}} \sim \int d^D r' (u(r') - u(r)) / (r - r')^{D+\alpha}$, with $\alpha = 1$ and $D = 1$ [54, 55, 57–59]. A second important example is provided by the sliding of frictional interfaces or of localized shear bands in amorphous materials [60–63]. Here, if inertia, velocity weakening or visco-elastic effects can be neglected, the dynamics is depinning-like with $D = 2$ and $\alpha = 1$.

The presence of long range elasticity does not change the qualitative picture of depinning given above, but for $\alpha < 2$ the value of the exponents β, ζ, τ and σ are modified; for $\alpha \geq 2$ short range exponents remain correct. Also, long range interactions can trigger distant weak spots to yield, leading to avalanches with disconnected pieces (see Fig. 1), called clusters. Their sizes, distances and extensions display power law behaviors as for the full avalanche, but with new exponents.

Note that many physical systems self-organize at their depinning transitions – naturally exhibiting an emergent scale invariant avalanche behavior and fractal front geometries. For example, in magnets, the weak but long-range magnetic dipole fields lead to *demagnetizing* forces [3, Sec. 8.2] that decrease the effective driving force as the front advances. Theoretical depinning models add an extra parabolic term to Eq. (2) in order to model this self-organization.

In section IV we will explain the relationship between avalanches below f_c , stationary flow above f_c , and the fractal structure of the interface at f_c , and how these properties are affected by long-range interactions.

C. Plasticity in amorphous materials

Other disordered systems display out of equilibrium phase transitions induced by an external drive. For example, a yielding transition is observed in foams, emulsions and metallic glasses when a stress, Σ , is applied. For a small stress these materials deform as solids, but for stresses Σ above a yield stress Σ_c they flow as liquids. In the liquid phase, the strain rate vanishes non-linearly [64, 65], $\dot{\epsilon} \sim (\Sigma - \Sigma_c)^\beta$. This behavior is similar to depinning (albeit with a larger flow exponent β), but here the system exhibits generic scale invariance. Scale invariant avalanches start well below Σ_c .

In the solid phase one observes plastic instabilities, called shear transformations [66], involving irreversible rearrangements of few bubbles or droplets. As illustrated in Fig. 4C, this local rearrangement induces a large, complex nearby rearrangement and a far-field power-law decay. This stress redistribution then can trigger other shear transformation zones that are kicked above their stability threshold.

Thus, as in depinning, this first instability can be the epicenter of an avalanche [67, 68]. The connection with the depinning transition can be made explicit considering the growth

of local strain $\epsilon(r, t)$ at a given stress Σ . Its evolution can be written [69] in the form of Eq. (2) for elastic interfaces driven with a force f . A crucial difference between yielding and depinning concerns the far-field kernel, which is of Eshelby type and not only features long range decay, but also¹ is non-monotonic [70, 71]. For example in 2D the elastic kernel can be written as

$$f_{el}[\epsilon(r, t)] \sim \int dr \frac{\cos 4\phi}{r^2} \delta\epsilon \quad (3)$$

Here, r is the distance from the shear transformation, ϕ the angle associated to the position \vec{r} , and f_{el} is the component of the stress tensor projected on the direction of the applied shear.² The presence of the positive and negative interactions from the cosine term is what makes f_{el} non-monotonic [43] – the transition increases the stresses for some neighbors, and decreases the stress for others. Indeed, after a plastic instability, the stress redistribution is on average zero: some regions see their stress increase, while in others the stress diminishes. This effect does not occur for the pandemic model or for the depinning transition, where the motion of a region of the interface can only destabilize other regions. For a yielding amorphous material, the stress that a given spot feels in time rises and falls, so that survival without going unstable becomes increasingly unlikely for the particularly weak spots. In section III we will see that the resulting *pseudogap* in the probability of regions ready to yield gives scale-invariant avalanches in the entire yielding solid phase – the system shows generic scale invariance.

D. Elasto-plastic models of depinning and yielding

Models of depinning and plastic yielding (sections IIB and IIC) often involve coupled networks of sites that each slip or jump to new configurations when pushed by one another or an overall stress field. Coupled block-spring models were introduced in the study of earthquakes by Carlson and Langer [73] without explicit disorder. We can model a depinning system with a D -dimensional lattice of blocks connected by springs, moving in a vertical direction u perpendicular to the lattice. We add a force threshold $\sigma_i^y = -f_{\text{dis}}(u_i, r_i)$ to each block that depends randomly on its vertical position, and have each block move by one unit, $u_i \rightarrow u_i + 1$, when it goes unstable. This produces a kick that can destabilize

¹ Monotonic, or ‘abelian’ interactions, also lead to *no-passing* theorems with fascinating implications [34, 43].

² A more realistic description of plastic interactions is tensorial [72], yet the scalar approximation described in the main text does not affect critical properties near the transition.

one or more of its neighbors, triggering an avalanche. Adding longer range springs with strength $G_{ij} \sim (r_i - r_j)^{-(1+\alpha)}$ gives us a long-range depinning model, and adding springs $G_{ij} = \cos(4\phi)/(r_i - r_j)^2$ gives us a model of yielding in amorphous materials [70, 71, 74, 75]. We shall return to this class of models again when we discuss mean-field theories of depinning in sections IV A and V A.

E. Jamming transition

How can a crowded, dense collection of particles manage to move and avoid each other as they are sheared? This question is relevant for the glass transition (when a liquid becomes an amorphous solid), the study of the flow of pedestrians [76] or (unexpectedly) the optimization of neural networks [77]. Initially it was motivated by granular materials, which can be solid or liquid depending on density and shear stress. They present a yield stress Σ_c separating these two phases, which for cohesionless materials must be proportional to the pressure p (the only stress scale in the problem) [78]. From the ratio $\mu_c = \Sigma_c/p$, one obtains the angle of repose $\Theta_c = \arctan \mu_c$, at which a layer of sand stops flowing. The stress ratio μ_c and the resulting angle of repose¹ Θ_c determines a critical point. For angles just above Θ_c , flow can occur despite the material being almost as dense as in the solid phase. Yet to avoid each other, the motion of the particles must be very cooperative [84–86] with long-range correlations or ‘eddies’, as illustrated in Fig. 2A. Also, the flow curve is singular at μ_c [78, 87–89] as illustrated in Fig. 2B. For example in dense suspensions $\mu(\mathcal{J}) - \mu_c \sim \mathcal{J}^\beta$, where $\mathcal{J} \equiv \eta_0 \dot{\epsilon}/p$ is a dimensionless ratio of the shear rate $\dot{\epsilon}$, the viscosity η_0 of the suspending fluid, and the particle pressure p (see section V B).

Progress was made by considering an ideal system: frictionless particles with repulsive, finite-range interactions (e.g., slippery rubber balls) [90, 91]. Imagine their positions to be initially random, then moved to locally minimize the energy. As illustrated in Fig. 3, for a large enough initial packing fraction of particles, this procedure leads to an amorphous solid, similar to a structural glass. For a small density, it leads to a gas of particles. At some threshold value ϕ_c , the particles are barely touching (a good model of granular materials) [92]. Key findings at ϕ_c are that (i) there exists a $\mu_c \approx 0.05$ below which the material is

¹ As mentioned above, sandpiles of frictional particles present two characteristic angles: Θ_c where flow stops, and $\Theta_{\text{start}} > \Theta_c$ where flow starts [3, 4, 79–83].

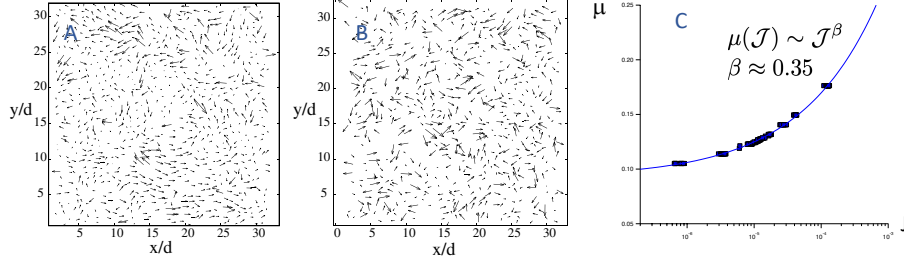


FIG. 2. **Jamming:** Critical properties of experimental granular flows. Fluctuating velocity of particles at the free surface of a granular flow in an inclined plane geometry of angle (a) 21° degree close to $\Theta_c = 20^\circ$, showing long-range spatial correlations and (b) far away from it $\Theta = 26^\circ$, where the flow is faster, less dense, and where these correlations are absent. From [[84]]. (c) Macroscopic friction coefficient μ versus dimensionless shear rate \mathcal{J} for different layer thicknesses h , showing an exponent $\beta \approx 0.35$. This experiment is performed in a drum geometry with short-range electrostatic repulsion between suspended particles, to ensure that they are effectively frictionless. We shall study the singular flow rates produced by the avalanches for depinning, yielding, and jamming in Secs. IV, V B, and VI B. From [[89]].

solid [93, 94]. For $\mu > \mu_c$, flow occurs and the flow curve is singular, capturing quantitatively the experimental results of Fig. 2C. (ii) Avalanches are observed for $\mu < \mu_c$, as shown in Fig. 3C [95]. (iii) Some structural properties display singular behavior. In particular, the distribution $P(f)$ of contact forces f , or the distribution $g(h)$ of interstices between particles, are characterized by non-trivial exponents at small arguments [96]:

$$P(f) \sim f^\theta \quad \text{with } \theta \approx 0.44, \quad (4)$$

$$g(h) \sim h^{-\gamma} \quad \text{with } \gamma \approx 0.38. \quad (5)$$

III. INSTABILITY THRESHOLDS AND STABILITY

Avalanches are triggered at weak spots, where an abrupt nonlinear response is triggered by an increasing field. More generally, amorphous and disordered materials allow for low-energy local rearrangements that can have a distribution $P(z)$ of excitations whose threshold force is z . It has long been known that systems like Coulomb glasses [97] and spin glasses [98] will excite those rearrangements with the lowest energies to optimize the interaction energies

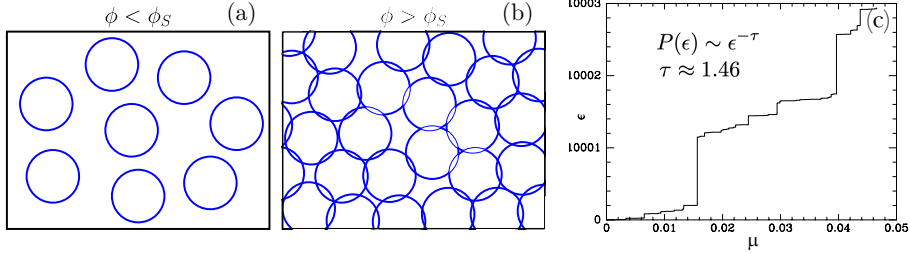


FIG. 3. (a) Unjammed assembly of particles at low packing fraction $\phi < \phi_c$ (b) Jammed packing with $\phi > \phi_c$. (c) At ϕ_c , as the stress anisotropy μ is increased, the strain ϵ displays a devil staircase: there are sequence where no rearrangements occur (horizontal line) followed by sudden jumps in strain or ‘avalanches’ that are power-law distributed. We will associate the presence of such a crackling phase with its marginal stability. From Ref. [95].

in finding the ground state. This removes many of the lowest energy excitations, leaving a density $P(z)$ of excitations that vanishes as a power law,

$$P(z) \sim z^{\theta_y}, \quad (6)$$

as the local excitation energy z goes to zero. Such a vanishing density is called a *pseudo-gap* (to distinguish it from a hard gap with no excitations in a finite energy range). Since then, it was realized that this situation is common, and affects both avalanches and stationary flows when they occur for large forcing.

A. Nature of excitations in the systems considered

Excitations correspond to nearly unstable rearrangements of the material. In magnetic systems, they are spins that are weakly polarized [98]. In elastic manifolds, they correspond to small portions of the interface. Here we focus on systems with long-range interactions, in which the notion of excitations turns out to be more crucial.

Amorphous solids: As discussed above, instabilities in that case are shear transformations, illustrated in Fig. 4(b). Here z is the increment of shear stress that will trigger an instability of a shear transformation zone, and $P(z)$ is the density of zones with trigger stress z . As briefly mentioned in Sec. II C, the non-monotonicity in the long-range interactions between transformations leads to a local stress history that varies both up and down as the material is plastically deformed, depleting the density of the lowest threshold transforma-

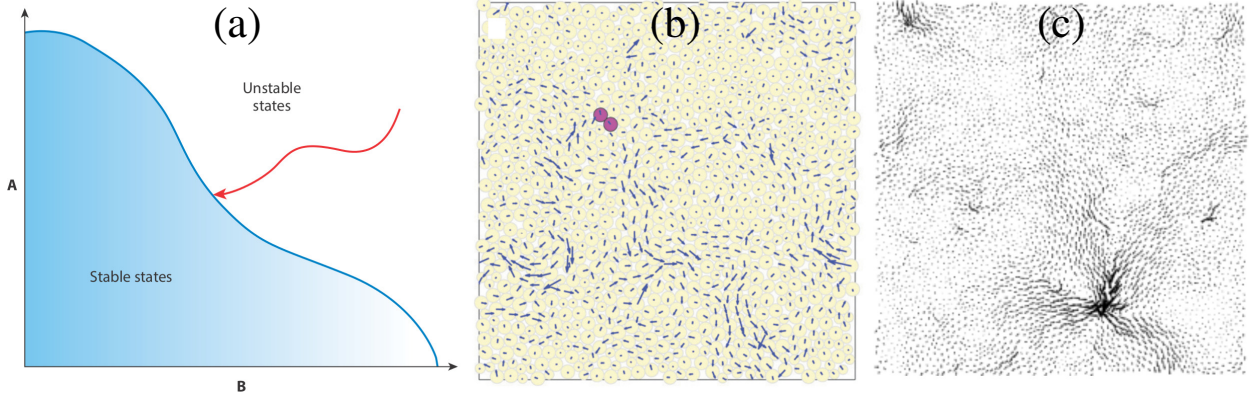


FIG. 4. (a) Schematic stability diagram in configuration space. A and B are observables characterizing the configurations visited. The full black line corresponds to marginal stability: It separates regions in which excitations are stable and unstable, respectively. The arrow illustrates a dynamical trajectory of a system that is cooling from an initial high temperature phase by stepwise relaxation of individual elementary excitations. When the system reaches the marginality line, the excitations become stable. If these excitations are the main drive of the dynamics, the system slows down very rapidly as it enters into the stable region and freezes very close to the marginal stability line. There, low-energy excitations are abundant, and rich dynamics, such as crackling noise, can occur. From Ref. [102]. (b) Elementary excitation corresponding to the opening of a single contact in a packing of hard discs. From Ref. [96]. (c) A shear transformation in an amorphous solid made of soft compressed particles. From Ref. [103].

tion zones. As in the equilibrium systems, sheared amorphous solids are found [99, 100] to displays a pseudo-gap, with $P(z) \sim z^{\theta_y}$. Interestingly, θ_y varies continuously under loading [101]. The condition $\theta_y > 0$ can be obtained from a stability argument [100]. Assume that $\theta_y = 0$ such that $P(x=0) = P_0 > 0$. Consider a shear transformation occurring at the origin, leading to a kick of stress of order $\Delta\Sigma(r) \sim r^{-d}$ at a distance r . The probability that a region of unit area displays an instability in response to this kick is $\sim \Delta\Sigma(r)P_0$. In a system of size L , the total number of new instabilities R_0 is then obtained by integration: $R_0 \sim P_0 \int_{r < L} \Delta\Sigma(r) r^{d-1} dr \sim \ln(L)$. This result implies that an individual plastic events always completely destroy the system (since $R_0 \gg 1$), with probability one. We know from experience that amorphous solids are stable to such local perturbations, thus implying $\theta_y > 0$.

Packings of frictionless hard spheres: These systems are *isostatic*: they just have enough contacts to ensure the stability of the material [104]. Under loading undeformable particles, rearrangements can only occur when a contact force goes to zero, leading to the opening of a contact and to a global motion of all particles called a ‘floppy mode’. An example of such an excitation is shown in Fig. 4(b). This motion stops when a new contact is formed. This process gives a kick of stress in the entire system, which can in turn trigger the opening of new contacts. The magnitude of the kick can be shown to be proportional to the displacement along the floppy mode before a new contact is formed, which occurs when a small gap between nearly touching particles closes. Thus, this distance is controlled by the distribution $g(h) \sim h^\gamma$ of gaps. Furthermore, the probability that a kick of given magnitude opens a new contact is controlled by the distribution of small forces $P(f) \sim f^\theta$. Requiring stability, i.e. that the number of new excitations triggered by a single one does not diverge in the thermodynamic limit (i.e. $R_0 \leq 1$), can be shown to imply [105]:

$$\gamma \geq 1/(2 + \theta) . \quad (7)$$

As described below, infinite range interactions (independent of distance) imply [102] a saturation of Eq. (7), $\gamma = 1/(2 + \theta)$, in agreement with numerical estimates of γ and θ . A great success of replica theory applied to the jamming transition is the computation of $\theta \approx 0.42$ and $\gamma \equiv 1/(2 + \theta) \approx 0.41$ in infinite dimensions [106]. These exponents agree well with simulations in finite dimensions [96, 107], as perhaps expected from numerical evidence [108, 109] that the upper critical dimension is $D_{uc} = 2$ for frictionless jamming.

B. Pseudo-gaps imply crackling noise

Stability arguments do not exclude the possibility that the density of excitations presents a hard gap (and strictly no rearrangements for a finite range of loading). Even if gapped configurations exist, they are not found in practice. Fig. 4(a) gives a pictorial illustration as to why it is so: for some systems and dynamics the system essentially stops as soon as it becomes stable, leading to a gapless marginal state. In mean-field spin glasses for example, it can be shown that finding gapped configurations is a NP complete problem [110].

The existence of a pseudo-gap implies that the rearrangements must be collective – avalanche like, with an initial rearrangement triggering at least some large events, lead-

ing usually to what we call crackling noise, without tuning or self-organizing to a critical point. Following [[102]], consider for example an amorphous solid of volume N , and assume that Eq. (6) applies. During an adiabatic loading, there will be periods without plasticity: their magnitude $\delta\Sigma$ is given by z_{min} , the stability of the least stable excitation. Standard extreme value statistics arguments [99, 111] lead to the typical value $z_{min} \sim N^{-1/(1+\theta_y)} \gg \frac{1}{N}$. It implies that the rate of plastic events is sub-extensive: a system twice as large does not display twice as many plastic events. Assume that no crackling occurs: then for local excitations, a plastic event involves $\mathcal{O}(1)$ excitations and thus dissipates an energy $\mathcal{O}(1)$, which is independent of N . For a global change of stress $\Delta\Sigma$, the energy dissipated is thus $\sim \Delta\Sigma/\delta\Sigma \sim N^{1/(1+\theta_y)} \ll N$, i.e. it is sub-extensive. Thus, in the absence of crackling, dissipation per unit volume must vanish in the thermodynamic limit. Plastic materials displaying a finite density of dissipation (which we expect to be the generic situation for disordered materials) must then display crackling. In particular for dissipation to be extensive, one must have $\langle S \rangle \sim N^{\theta_y/(1+\theta_y)}$.

We return to infinite range interactions (such as frictionless hard spheres in any dimensions, or the SK model of spin glasses). In that case, it can be shown that if inequalities like Eq. (7) are not saturated [102], then an excitation has a vanishing probability to trigger a second one in the thermodynamic limit: crackling cannot occur. But we have seen before that crackling noise must occur (to allow for an extensive dissipation), thus our hypothesis is incorrect: we conclude that the bound in Eq. (7) must be saturated when infinite-range interactions are present. Note that saturation does not occur for power-law interactions, e.g. in amorphous solids.

Ultimately, this approach leads to a classification of glassy systems based on the range of the interaction of their excitations. If sufficiently long-range and non-monotonic, then a pseudo-gap must be present, and crackling occurs. Instead for short-range interactions, crackling occurs only at a critical point and not in the entire glassy phase. As we shall see below, the pseudo-gap exponent also characterizes the flowing phase, when it exists.

IV. THEORETICAL RESULTS: DEPINNING

A. Mean-field theory of depinning

Depinning (see Eq. (2)) is characterized by the competition between a decaying elastic force, $f_{\text{el}} \sim \int d^D r (u(r') - u(r))/|r - r'|^{D+\alpha}$ that flattens the interface and a disorder force of the $D + 1$ dimensional medium that tries to roughen it. Dimensional analysis can help to determine the result of this competition, if we assume that the interface is self-affine, namely that after a dilatation $x \rightarrow bx$, its transverse fluctuations grow as $b^\zeta u(x)$. After the dilatation, the elastic force is rescaled as $b^{\zeta-\alpha}$ for $\alpha < 2$ (for shorter-ranged forces it turns out to scale as $b^{\zeta-2}$) and the short-range disorder force turns out to be rescaled as $b^{D/2-\zeta/2}$. Using a Flory type of argument one has to balance the two forces in order to estimate the roughness exponent [112, 113]. Thus, the interface results flat ($\zeta = 0$) at the upper critical dimension $D_{\text{uc}} = 2\alpha$ for $\alpha < 2$, matching nicely with the value $D_{\text{uc}} = 4$ above $\alpha > 2$.

Above D_{uc} disorder is not able to roughen the interface, which turns out to slide with a velocity linear in the force above threshold ($\beta = 1$), and display mean field avalanches ($\tau = 3/2$, $\sigma = 1/2$, and $z = \alpha$), as discussed below. Below $D_{\text{uc}} = 2\alpha$, the interfaces are rough ($\zeta > 0$), the velocity grows with a power β less than one, with avalanche exponents τ , σ , and z smaller than those in mean-field.

This Flory argument correctly predicts D_{uc} , a result that can be also obtained treating the disorder as a perturbation [41, 114–116]. Unfortunately both arguments fail in predicting the exact value of the exponents below D_{uc} . Indeed, for purely linear models, the Flory balance works perfectly at each length scale. However, any nonlinear terms will couple the different length scales, and thus demand a renormalization group approach.¹

A mean-field theory for depinning can be formed using the block-spring model of section IID, but having every pair of sites x_i and x_j connected by a spring $G_{ij} \equiv G/N$, with N the number of blocks. After each block slips, all blocks receive a kick (force increment) of G/N . Hence, the dynamics are precisely the same as that in the Bienaymé-Galton-Watson process we saw in the pandemic model. The value of the force f controls the parameter R_0 , which becomes critical ($R_0 = 1$) at $f = f_c$. Because all of the kicks are in the same direction, the interaction is monotonic, and there is no pseudogap. Above f_c a stationary

¹ In systems with ‘KPZ’-type nonlinearities Flory’s arguments do not work in any dimension. In this case it remains controversial if it exists an upper critical dimension above which interfaces are flat.

TABLE I. **Critical exponents and scaling relations** for depinning systems of D dimensional interfaces in $D + 1$ dimensions, assuming no nonlinearities of the qKPZ type and elastic forces $f_{\text{el}} \sim \int d^D r (u(r') - u(r))/|r - r'|^{D+\alpha}$. The last column shows one-loop functional renormalization group calculations [117–120] with $D_{\text{uc}} = \min(2\alpha, 4)$ and $\epsilon = D_{\text{uc}} - D$. Above D_{uc} behavior is mean-field. For $D < D_{\text{uc}}$, exponents are measured numerically with a precision at the second digit. Note that depinning models do not have a pseudogap, so $\theta_y = 0$.

Depinning	Observable	$D = 1$	$D = 1$	$D = 2$	FRG
exponent		$\alpha = 2$	$\alpha = 1$	$\alpha = 2$	$D = D_{\text{uc}} - \epsilon$
z	$t(L) \sim L^z$	1.43	0.77	1.56	$D_{\text{uc}}/2 - 2\epsilon/9$
ζ	$u(x) \sim x^\zeta$	1.25	0.39	0.75	$\epsilon/3$
τ	$P(S) \sim S^{-\tau}$	$\tau = 2 - \alpha/(D + \zeta)$			$3/2 - \epsilon/(3D_{\text{uc}})$
ν	$\xi \sim f - f_c ^{-\nu}$	$\nu = 1/(\alpha - \zeta)$			$2/D_{\text{uc}} + 4\epsilon/(3D_{\text{uc}}^2)$
β	$v \sim f - f_c ^\beta$	$\beta = \nu(z - \zeta)$			$1 - \epsilon/(9D_{\text{uc}})$

flow is present with a permanent fraction of unstable blocks $\sim |f - f_c|^\beta$, with $\beta = 1$.

B. Finite dimension and Functional RG

Table I gives a summary of exponents for the depinning of D -dimensional manifolds in $D + 1$ dimensions. The last three rows in the table give a set of scaling relations that allow one to express all the exponents in terms of two, ζ and z , valid below D_{uc} . For example, the velocity above threshold can be expressed as the ratio between avalanche displacement and avalanche duration, namely $v \sim \xi^\zeta / \xi^z \sim |f - f_c|^{-\nu(\zeta - z)}$, giving the equation for β . The last column in Table I gives one-loop functional RG (FRG) results for the exponents [117–120] close to the upper critical dimension. Two-loop [121–123] and three-loop calculations for the static problem are now available [124, 125].

The RG approach captures the large-scale scale invariant properties of a population of configurations. The traditional RG studies the flow in a space of parameters (field H , temperature T , ...) which yield an effective coarse-grained free energy; the free energy encodes the Gibbs weight of different configurations. Here, the weight of the dynamical trajectories is encoded into the Martin-Siggia-Rose action, which averages trajectories over

disorder. The resulting RG involves a full function: the force-force disorder correlator, $\Delta(u - u')$, where u, u' are two different positions of the center of mass of the interface. The fixed point Δ^* can be computed by FRG as a perturbation in $\epsilon = D_{uc} - D$ and has a peculiar cusp at the origin $u = u'$ which has been experimentally measured [126]. Indeed, when an avalanche occurs, much of the interface is left pinned at the same position (same disorder), but the disorder force changes abruptly in the regions which have slipped forward (Fig. 1), leading to the cusp.

For physical systems in $D = 1$ and $D = 2$, the best estimation of depinning exponents come from numerical calculations [114, 127–132], summarized in the first two rows of Table I. The two-loop expansion [121–123, 133], however, settled a *qualitative* question — showing that the interface at thermal equilibrium has a different roughness and universality class from that of the interface at depinning. Even more surprisingly, FRG [115] is also able to describe the thermally activated slow dynamics of magnetic domain walls driven by a magnetic field much smaller than the critical force. Most of the predictions for this creep regime have been tested both experimentally [134, 135] and numerically [136]. See also the FRG results for the avalanche shape in section IV C.

Critical exponents are neither the only quantity of interest nor the simplest to observe in experiments [137, 138]. The value of the critical force f_c and its universal fluctuations [139–141] are important for applications. In the following we will see in some details some other important example of such observables.

C. The average avalanche time series

A longstanding challenge for the scaling theory of dynamical disordered systems was the rather symmetrical predictions for the average temporal shape [143, 144], which disagreed with a much larger asymmetry in experiments [1]. This eventually was explained as an effect of eddy currents [145]. Figure 5A shows the time-dependent mean front velocity during a mean-field magnetic avalanche in a thin magnetic film [142], avoiding the effects of eddy currents. Note the characteristic irregular, fractal shape – almost stopping several times. (If it had stopped, it would form a smaller avalanche – big avalanches are just smaller avalanches that did not stop a few times.) Note also the dashed curve – an average $V(t|T)$ over all the experimental avalanches whose durations T were similar to this one. The universal scaling

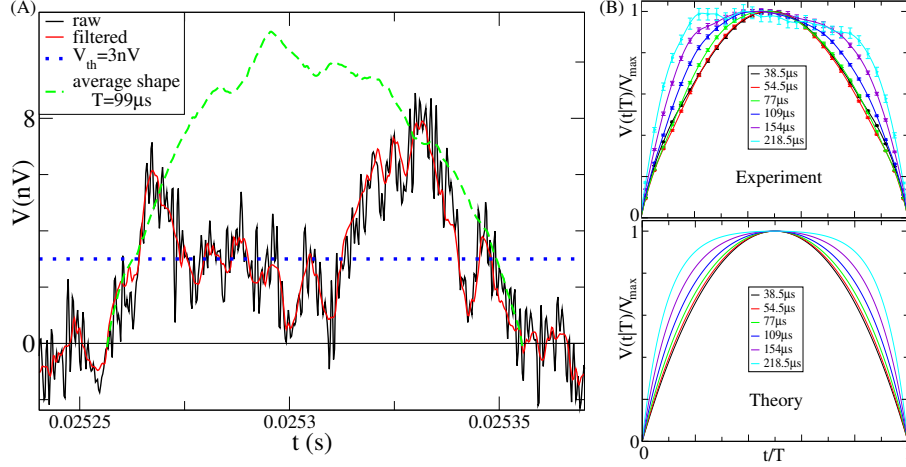


FIG. 5. **Avalanche, and average temporal shape**, from Ref. [[142]]. (A) Experimental signal during an avalanche (jagged), with noise filtered out (wavy), rather than using thresholding (dotted). The dashed line shows the signal $V(t/T)$ averaged over all avalanches of similar duration. (B) Average temporal shape in experiment and predicted by mean-field theory (Eq. (8)) for various avalanche durations.

prediction for this average shape is [1, 143]

$$V(t|T, r) = T^{d_f/z-1} \mathcal{V}(t/T, Tr^{z\nu}) = T \mathcal{V}(t/T, Tr) . \quad (8)$$

Figure 5B shows a scaling collapse of average avalanche shapes for different durations (top) and the universal scaling prediction from mean-field [142, 146] (bottom). The average shape is an inverted parabola for avalanches small compared to the cutoff $T_{\max} \sim r^{-z\nu} = 1/r$, and has an explicit analytical form for longer durations in mean-field theory (Fig. 5B).

The same functional RG methods we discussed in section IV B, remarkably, have been applied [147] to predict the average temporal shape both at fixed duration and fixed avalanche size for $D \leq D_{uc}$. They predict a slight skewing of the avalanches that nicely fits the measured shapes [144, 148], and also incorporate eddy currents into the scaling predictions [148, 149].

D. Clusters in avalanches with long-range interactions

As we saw in Fig. 1, avalanches in systems with long-range interactions can be disconnected into *clusters*. It is infeasible in most experiments to visualize avalanches one-by-

one[150], and naturally impossible to figure out after several avalanches which clusters came from which avalanches – we cannot directly find τ , σ , etc.

At moderate rates of strain, one can measure the statistics of clusters localized in space, which fortunately also display universal scaling [151]. For example their size S_c has a power law probability distribution $P(S_c) \sim S_c^{-\tau_c}$. The other avalanche exponents can be defined for clusters as well. A solid numerical conjecture predicts the value of cluster exponents in terms of the avalanche exponents [152]. For example the relation $\tau_c = 2\tau - 1$ should hold for $\alpha < 2$. One must note, though, that our analytical study of a simple epidemic model with long range dispersal does not show this behavior [153].

The key to this conjecture is the identification of a Bienaymé-Galton-Watson process describing the statistics of the cluster number [154]. This process has been clearly observed numerically for all $\alpha < 2$, but no proof of its existence yet exists. For $\alpha > 2$ the number of clusters is strongly suppressed; $\tau_c = \tau$ for forces of finite range. It is not yet clear how τ_c behaves for large, but finite values of α . A future challenge is to understand the origin of the Bienaymé-Galton-Watson process describing the cluster statistics.

V. THEORETICAL RESULTS: YIELDING TRANSITION

A. Mean field models of yielding

The mean-field version of the elasto-plastic block-spring models for the yielding transition (section IID) have non-monotonic interaction matrices G_{ij} with both positive and negative values that are randomly chosen with the same distribution and independent of i and j (infinite range). Let us call $z_i = \sigma_i^y - \sigma_i$, where σ_i and σ_i^y are respectively the shear stress and the yield stress of that block. When $z_i < 0$ the block yields, reducing all the other z_j by G_{ij}

In the *Hebraud-Lequeux* model [155], G_{ij} is assumed to follow a Gaussian distribution of variance $\sim N^{-1/2}$, where N is the number of blocks. As a result, each variable z_i is a sum of Gaussian random kicks, where the walk ends when the sum hits zero – a random walk with an absorbing condition at $z = 0$. After yielding, the site is reinserted at some finite positive z_i value. Solving this random walk problem, we find that the distribution $P(z)$ evolves until it vanishes linearly with $\theta_y = 1$. The flow curve is found to be singular at Σ_c , with $\beta = 2$.

Interestingly [156], the distribution of avalanches sizes depends on details of how the system is loaded. For realistic loading, $\tau \approx 1$.

In a more realistic mean-field model, the noise is not assumed to be Gaussian. It is still i.i.d. and thus has no spatial correlations, but the distribution of G_{ij} is chosen to satisfy that of the true propagator. For a propagator that vanishes with distance as a power-law, $P(G)$ is then power-law distributed [157]. In that case, z_i follows a *Levy flight* with a Levy coefficient $\mu = 1$. The pseudo-gap is still governed by an absorbing condition: it is found that after a quench at zero stress, $\theta_y = 1/2$ [158]. However, here θ_y continues to evolve as the system is strained; it starts by rapidly decreasing, and then increases. This has been observed in finite dimensional elasto-plastic models [101] and in molecular dynamics of amorphous solids [159, 160]. Flow curves are again singular, with $\beta = 1$ [161]. In this model, aging responses following a quench (a minimization of the energy from some random configuration at $t = 0$) can be computed [162], and are found to be similar to experimental ones.

B. Scaling theory for yielding

In this section we will provide a link between the avalanche physics at the mesoscale and the flow curve at the macroscale, for systems with non-monotonic long-range interactions (such as amorphous materials yielding under stress, section III).

Stationarity: Consider applying a quasi-static strain in a system of linear size L at the yielding transition. The stress Σ ramps up under increasing strain, and drops abruptly during avalanches. On average, these must cancel out [67, 99, 163]. An avalanche of size S will lead to a stress drop in the system that is proportional to $\delta\Sigma \sim \langle S \rangle / L^d$. The mean avalanche size is $\langle S \rangle \sim \int^{S_{\max}} S \times S^{-\tau} dS \propto S_{\max}^{2-\tau}$, where $S_{\max} \sim L^{d_f}$ is the largest avalanche that can fit into the system. The stress rise between avalanches is determined by the pseudogap in the distribution of threshold stresses. As discussed in section III, the weakest site will yield after the stress increases by $\sim L^{-d/(1+\theta_y)}$. Equating the average drop and the average increment, one obtains[69]:

$$\tau = 2 - \frac{\theta_y}{\theta_y + 1} \frac{d}{d_f} . \quad (9)$$

Dynamics in the flowing regime: As one approaches the critical stress Σ_c from above

in the flowing regime, there is a diverging length scale $\xi \sim (\Sigma - \Sigma_c)^\nu$. Below this length scale, both in depinning transitions [39] and in the yielding transition [69] one can roughly describe the motion as a continuously evolving collection of avalanches of spatial length ξ , covering space. The net strain rate $\dot{\epsilon}$ is the number of avalanches $\sim 1/\xi^d$ times the strain release $S \sim \xi^{d_f}$ per avalanche divided by the duration $T \sim \xi^z$ of these avalanches, hence $\dot{\epsilon} = S/(T\xi^d) \sim (\Sigma - \Sigma_c)^{\nu(d-d_f+z)}$. Hence the strain rate $\dot{\epsilon} \sim (\Sigma - \Sigma_c)^\beta$ grows with an exponent

$$\beta = \nu(d - d_f + z) . \quad (10)$$

Stress fluctuations: Continuing to view the flow as a superposition of avalanches of size S_{\max} spanning boxes of size $V = \xi^d$, each will lower the stress in its box by an amount $\delta\Sigma \sim S_{\max}/\xi^d \sim (\Sigma - \Sigma_c)^{\nu(d-d_f)}$. Making the common assumption that all quantities with the same units share the same scale near a critical point, we expect that the fluctuations of stress $\delta\Sigma$ on the scale ξ must be of order of the distance to threshold $\Sigma - \Sigma_c$, leading to [69, 163]:

$$\nu = 1/(d - d_f) . \quad (11)$$

Putting Eqs. (11) and (10) together, one obtains $\beta = 1 + z/(d - d_f) \geq 1$. Note that the scaling relations in Eqs. (9)–(11) should work in elasto-plastic models, particle based models, and real systems, as supported by observations [69, 74]. One must note that elasto-plastic models assume that elastic interactions propagate instantly, and sometimes give an unphysical value of $z < 1$ (leading to avalanche propagation faster than the speed of sound). In this case, we presume that $z = 1$ and the value of β in Eq. (10) should thus be larger in physical systems than in elasto-plastic models [161].

These scaling arguments can be extended to non-stationary situations [164] such as the slow creep flows [165] that follows a sudden increase of stress, to non-local phenomena [166] where $\xi \sim |\Sigma - \Sigma_c|^{-\nu}$ is found to characterize the length scale on which an obstacle or interface perturbs flow [167], and to finite temperatures [168, 169] that cause a “thermal rounding” of the flow curves, which becomes smooth near Σ_c .

VI. THEORETICAL RESULTS: JAMMING

A. Infinite-dimension calculations of avalanches

Avalanches are dynamical phenomena. Yet ‘equilibrium avalanches’ can be defined, by tilting the energy landscape continuously by adding a force or field, and tracking the position of the global minimum of the system [170]. It then displays jumps, whose statistics can be computed in infinite dimension using replica methods. Right at the jamming transition, this method was successfully used to compute $\tau = (3 + \theta)/(1 + \theta) \approx 1.41$ [171] in close agreement with numerical experiments for nonequilibrium avalanches in three dimensions [95].¹ The success of the mean-field approach arguably results from the infinite-range nature of excitations in this system [86].

A system of well-compressed particles (packed more densely than at the jamming threshold) should exhibit a yielding behavior as described in subsection II C. Replica theory of jamming predicts $\tau = 1$ for the rigid phase [171]. This mean-field result may not hold in three dimensions however, as the length scale of excitations rapidly decreases away from jamming [174], and spatial correlations are then presumably important.

B. Suspension and granular flows of frictionless particles

Much of the jamming literature has focused on frictionless particles, both numerically [175–179] and theoretically [180]. Friction is of course important for most of the applications of jamming – from soil engineering to pharmaceuticals to geophysics. It was recently realized that a class of suspensions displaying “shear thickening” display effectively frictionless particles at low stresses, but they become frictional at large stresses [181–184]. Controlled experimental systems with these properties have been designed [80, 89, 185, 186], allowing one to experimentally test scaling theories of flow for frictionless jamming.

Consider a frictionless packing at the critical stress anisotropy $\mu = \Sigma/p = \mu_c$. The first step of the theory consists of estimating the number of contacts δz that open if the

¹ It is known in the random-field Ising model that the universality class of the equilibrium system is different from that of the non-equilibrium, avalanche model at zero temperature. This has been shown in dimensions smaller than about 5.1 using remarkable non-perturbative functional renormalization-group calculations [172], and numerically in two dimensions [173]. Here, however, we are above the upper critical dimension, where non-equilibrium and equilibrium properties should be similar.

stress anisotropy is increased by $\mu - \mu_c$. One finds, by estimating the change of forces in the contacts induced by such a perturbation, and using that the distribution of small force follows $P(f) \sim f^\theta$, that [180]:

$$\delta z \sim (\mu - \mu_c)^{\frac{2+2\theta}{3+\theta}}. \quad (12)$$

Using this, one can use mechanical considerations to compute how an infinitesimal applied strain $\delta\epsilon$ at the boundary moves particles relatively to each other, by some amount δr called the non-affine displacement. Defining $\mathcal{L} \equiv \delta r / \delta\epsilon$, one finds [180]:

$$\mathcal{L} \sim \delta z^{-\frac{2+\theta}{1+\theta}}. \quad (13)$$

The overall viscosity of such a suspension is proportional to the dissipated power, which grows as the square of the particle velocities, and is thus proportional to \mathcal{L}^2 . The viscous number \mathcal{J} is inversely proportional to this viscosity, thus $\mathcal{J} \equiv \eta_0 \dot{\epsilon} / p \sim \mathcal{L}^{-2}$. Together with Eqs. (12) and (13), one obtains the flow curve:

$$\mu - \mu_c \sim \mathcal{J}^{\frac{3+\theta}{8+4\theta}} \approx \mathcal{J}^{0.35}, \quad (14)$$

in agreement with experiments, as shown in Fig. 2. Several diverging length scales are predicted at the transition [86]; one of these (the divergence of non-local effects) has been favorably tested [89].

Note that this theory is mean-field in nature, as it neglects spatial correlations that could occur e.g. in the structure. Its quantitative agreement with finite dimensional numerical studies [180] and experiments [89] again underlines the mean-field character of the jamming transition for frictionless particles, where excitations have infinite range interactions at threshold. This situation does not hold for frictional particles, where other exponents are found [187, 188] and spatial correlations are relevant [189]. An additional complexity is that in the presence of friction, the flow curve is non-monotonic and the transition is first order close to the critical point [80–82, 189].

VII. CONCLUSION AND OPEN QUESTIONS

We have described the closely intertwined physics of avalanches, the stability of the rigid phase, and stationary flows in a variety of disordered systems. Scaling concepts are the key to building such a unifying description. The renormalization group inspires these scaling

descriptions, but they are useful even in cases where a RG procedure has not (yet) been developed. We conclude by listing a few open problems in this field:

RG description of the yielding transition: Although the jamming transition of hard particles appears to be mean-field in character, the yielding transition of amorphous materials appears more subtle. Currently, there is no analytical approach to compute exponents in that case (except for avalanche exponents in conditions where a narrow shear band appears, where a mean-field description may apply [60–63]).

Avalanches and first order transitions: Systems often exhibit avalanche precursors before abrupt changes in behavior. The abrupt change in behavior is due to a non-monotonic flow curve: the same force (stress) can lead to different velocities (strain rate). Quasi-brittle materials exhibit power-law fracture precursors under tension [18] before they fracture into two. This also occurs in complex fluids (such as loosely connected colloidal gels) and earthquakes (where frictional forces acting on the fault can decrease with sliding velocity [190]). Inertia can also lead to such flow curves in depinning problems [5, 191] and in amorphous solids [68, 192]. Velocity (or strain-rate) weakening can make the transition between a rigid and flowing phase first order and hysteretic, possibly destroying avalanches. Recent work on frictional interfaces suggests that avalanches persist in that situation (although their statistics change), and act as nucleation centers for system-spanning events [193]. In that view, the avalanche size diverges at some threshold stress, beyond which the rigid material is unstable to the presence of a large nucleus of flowing material. How generic these results are remain to be seen.

Nucleation of failure: This contribution focuses on stationary flow in disordered materials. Another important question is how these materials break as the loading continuously increases. For amorphous solids, this usually occurs by forming a shear-band where plastic strain localizes. Some have argued that the shear band nucleates in a process similar to that of the random-field Ising model [160, 194], or fracture [195]; others suggest it is governed by linear stability considerations [196]. Numerical studies [197] report very slowly-decaying finite-size effects that remain to be understood.

Yielding at finite temperature T and the glass transition: we focused on the yielding transition at $T = 0$. At finite temperature, the flow curve loses its singular behavior, in a stress interval around Σ_c that vanishes as a power law of T [168, 169]. Such a ‘thermal rounding’ behavior can be captured by mean field calculations or scaling arguments [168].

Yet, a spatial description of thermal avalanches triggered by rare activated events is still missing. It may be very relevant to understand the collective dynamics that occurs near the glass transition [198].

ACKNOWLEDGMENT

JPS would like to acknowledge the support of NSF DMR-1719490. MW acknowledges support from the Simons Foundation Grant (No. 454953 Matthieu Wyart) and from the SNSF under Grant No. 200021-165509.

-
- [1] J. P. Sethna, K. A. Dahmen, and C. R. Myers, Crackling noise, *Nature*. **410**, 242–250, (2001).
 - [2] J. P. Sethna, K. A. Dahmen, and O. Perković. Random-field models of hysteresis, <http://arxiv.org/abs/cond-mat/0406320>. In *The Science of Hysteresis, Vol. II*, pp. 107–179. Academic Press, (2006).
 - [3] S. Zapperi, *Crackling noise: Statistical physics of avalanche phenomena*. (Oxford University Press, Oxford, 2022).
 - [4] S. R. Nagel, Instabilities in a sandpile, *Rev. Mod. Phys.* **64**, 321–325 (Jan, 1992). doi: 10.1103/RevModPhys.64.321. URL <https://link.aps.org/doi/10.1103/RevModPhys.64.321>.
 - [5] D. Fisher, K. Dahmen, S. Ramanathan, and Y. Ben-Zion, Statistics of Earthquakes in Simple Models of Heterogeneous Faults, *Phys. Rev. Lett.* **78**(25), 4885–4888, (1997). doi: 10.1103/PhysRevLett.78.4885.
 - [6] A. P. Mehta, K. A. Dahmen, and Y. Ben-Zion, Universal mean moment rate profiles of earthquake ruptures, *Physical Review E*. **73**(5), 056104, (2006).
 - [7] E. A. Jagla, F. P. Landes, and A. Rosso, Viscoelastic Effects in Avalanche Dynamics: A Key to Earthquake Statistics, *Phys. Rev. Lett.* **112**(17), (2014). doi: 10.1103/PhysRevLett.112.174301.
 - [8] L. de Arcangelis, C. Godano, J. R. Grasso, and E. Lippiello, Statistical physics approach to earthquake occurrence and forecasting, *Physics Reports*. **628**, 1–91, (2016). doi:

- 10.1016/j.physrep.2016.03.002.
- [9] J. P. Sethna, Statistical mechanics - Crackling crossover, *Nature Physics (News and Views)*. **3**, 518–519, (2007).
 - [10] G. Durin and S. Zapperi. The science of hysteresis: Physical modeling, micromagnetics and magnetization dynamics, vol. ii, ch. iii (the barkhausen effect), (2006).
 - [11] V. Berejnov and R. E. Thorne, Effect of transient pinning on stability of drops sitting on an inclined plane, *Phys. Rev. E*. **75**, 066308 (Jun, 2007). doi:10.1103/PhysRevE.75.066308. URL <https://link.aps.org/doi/10.1103/PhysRevE.75.066308>.
 - [12] J. P. Sethna, Crackling wires, *Science (Perspective)*. **318**, 207–208, (2007).
 - [13] N. Friedman, A. T. Jennings, G. Tsekenis, J.-Y. Kim, M. Tao, J. T. Uhl, J. R. Greer, and K. A. Dahmen, Statistics of dislocation slip avalanches in nanosized single crystals show tuned critical behavior predicted by a simple mean field model, *Physical review letters*. **109** (9), 095507, (2012).
 - [14] J. P. Sethna, M. K. Bierbaum, K. A. Dahmen, C. P. Goodrich, J. R. Greer, L. X. Hayden, J. P. Kent-Dobias, E. D. Lee, D. B. Liarte, X. Ni, K. N. Quinn, A. Raju, D. Zeb Rocklin, A. Shekhawat, and S. Zapperi, Deformation of crystals: Connections with statistical physics, *Annual Review of Materials Research*. **47**, 217–246, (2017). doi: 10.1146/annurev-matsci-070115-032036. URL <http://www.annualreviews.org/doi/full/10.1146/annurev-matsci-070115-032036>.
 - [15] X. Ni, H. Zhang, D. B. Liarte, L. W. McFaul, K. A. Dahmen, J. P. Sethna, and J. R. Greer, Yield precursor dislocation avalanches in small crystals: The irreversibility transition, *Phys. Rev. Lett.* **123**, 035501 (Jul, 2019). doi:10.1103/PhysRevLett.123.035501. URL <https://link.aps.org/doi/10.1103/PhysRevLett.123.035501>.
 - [16] S. Papanikolaou, D. M. Dimiduk, W. Choi, J. P. Sethna, M. D. Uchic, C. F. Woodward, and S. Zapperi, Quasi-periodic events in crystal plasticity and the self-organized avalanche oscillator, *Nature*. **490**(7421), 517–521 (10, 2012). URL <http://dx.doi.org/10.1038/nature11568>.
 - [17] F. F. Csikor, C. Motz, D. Weygand, M. Zaiser, and S. Zapperi, Dislocation avalanches, strain bursts, and the problem of plastic forming at the micrometer scale, *Science*. **318**(5848), 251–254, (2007).
 - [18] A. Shekhawat, S. Zapperi, and J. P. Sethna, From damage percolation to crack nucleation

- through finite-size criticality, *Physical Review Letters*. **110**, 185505, (2013).
- [19] S. Tewari, D. Schiemann, D. J. Durian, C. M. Knobler, S. A. Langer, and A. J. Liu, Statistics of shear-induced rearrangements in a two-dimensional model foam, *Physical Review E*. **60** (4), 4385, (1999).
 - [20] M. Cieplak and M. O. Robbins, Dynamical transition in quasistatic fluid invasion in porous media, *Physical review letters*. **60**(20), 2042, (1988).
 - [21] J. Ortín and S. Santucci. Avalanches, Non-Gaussian Fluctuations and Intermittency in Fluid Imbibition. In eds. E. K. Salje, A. Saxena, and A. Planes, *Avalanches in Functional Materials and Geophysics*, pp. 261–292. Springer International Publishing, Cham, (2017). ISBN 978-3-319-45610-2 978-3-319-45612-6. doi:10.1007/978-3-319-45612-6_12.
 - [22] M. Kuntz, P. Houle, and J. P. Sethna. Crackling noise. <http://SimScience.org/crackling/>, (1998).
 - [23] M. Alava, M. Dubé, and M. Rost, Imbibition in disordered media, *Advances in Physics*. **53** (2), 83–175, (2004). doi:10.1080/00018730410001687363. URL <https://doi.org/10.1080/00018730410001687363>.
 - [24] D. Pines, J. Shaham, M. A. Alpar, and P. W. Anderson, Pinned Vorticity in Rotating Superfluids, with Application to Neutron Stars[†]), *Progress of Theoretical Physics Supplement*. **69**, 376–396 (03, 1980). ISSN 0375-9687. doi:10.1143/PTP.69.376. URL <https://doi.org/10.1143/PTP.69.376>.
 - [25] E. D. Lee, B. C. Daniels, C. R. Myers, D. C. Krakauer, and J. C. Flack, Scaling theory of armed-conflict avalanches, *Phys. Rev. E*. **102**, 042312 (Oct, 2020). doi: 10.1103/PhysRevE.102.042312. URL <https://link.aps.org/doi/10.1103/PhysRevE.102.042312>.
 - [26] N. Friedman, S. Ito, B. A. Brinkman, M. Shimono, R. L. DeVille, K. A. Dahmen, J. M. Beggs, and T. C. Butler, Universal critical dynamics in high resolution neuronal avalanche data, *Physical review letters*. **108**(20), 208102, (2012).
 - [27] J. M. Beggs and D. Plenz, Neuronal avalanches in neocortical circuits, *Journal of neuroscience*. **23**(35), 11167–11177, (2003).
 - [28] L. Salminen, A. Tolvanen, and M. J. Alava, Acoustic emission from paper fracture, *Physical Review Letters*. **89**(18), 185503, (2002).
 - [29] P. A. Houle and J. P. Sethna, Acoustic emission from crumpling paper, *Physical Review E*.

- 54**, 278–283, (1996).
- [30] E. M. Kramer and A. E. Lobkovsky, Universal power law in the noise from a crumpled elastic sheet, *Physical Review E*. **53**(2), 1465, (1996).
 - [31] Q. Michard and J. Bouchaud, Theory of collective opinion shifts: from smooth trends to abrupt swings, *Eur. Phys. J. B*. **47**, 151–159, (2005). URL <https://doi.org/10.1140/epjb/e2005-00307-0>.
 - [32] I.-J. Bienaymé, De la loi de multiplication et de la durée des familles, *Oc Philomat Paris Extr. Sér.* **5**(37-39), 4, (1845).
 - [33] H. W. Watson and F. Galton, On the Probability of the Extinction of Families., *The Journal of the Anthropological Institute of Great Britain and Ireland*. **4**, 138, (1875). doi: 10.2307/2841222.
 - [34] J. P. Sethna, K. Dahmen, S. Kartha, J. A. Krumhansl, B. W. Roberts, and J. D. Shore, Hysteresis and hierarchies - dynamics of disorder-driven 1st-order phase-transformations, *Physical Review Letters*. **70**, 3347–3350, (1993).
 - [35] J. P. Sethna, Power laws in physics, *Nature Reviews Physics*. **4**, 501–503 (Jul, 2022). doi: 10.1038/s42254-022-00491-x. URL <https://rdcu.be/cSbCZ>.
 - [36] Y.-J. Chen, S. Zapperi, and J. P. Sethna, Crossover behavior in interface depinning, *Phys. Rev. E*. **92**, 022146, (2015). doi:<http://dx.doi.org/10.1103/PhysRevE.92.022146>. URL <http://link.aps.org/doi/10.1103/PhysRevE.92.022146>.
 - [37] P. Bak, C. Tang, and K. Wiesenfeld, Self-organized criticality: An explanation of the 1/f noise, *Physical review letters*. **59**(4), 381, (1987).
 - [38] S. Zapperi, K. B. Lauritsen, and H. E. Stanley, Self-organized branching processes: Mean-field theory for avalanches, *Phys. Rev. Lett.* **75**, 4071–4074 (Nov, 1995). doi: 10.1103/PhysRevLett.75.4071. URL <https://link.aps.org/doi/10.1103/PhysRevLett.75.4071>.
 - [39] D. S. Fisher, Collective transport in random media: from superconductors to earthquakes, *Physics Reports*. **301**(1-3), 113 – 150, (1998). ISSN 0370-1573. doi:10.1016/S0370-1573(98)00008-8. URL <http://www.sciencedirect.com/science/article/pii/S0370157398000088>.
 - [40] M. Kardar, Nonequilibrium dynamics of interfaces and lines, *Physics Reports*. **301**(1-3), 85–112, (1998). doi:10.1016/S0370-1573(98)00007-6.

- [41] A. Larkin, Model for pinning of vortex lattices, *Sov. Phys. JETP*. **31**, 784, (1970).
- [42] D. S. Fisher, Sliding charge-density waves as a dynamic critical phenomenon, *Phys. Rev. B*. **31**(3), 1396–1427, (1985). doi:10.1103/PhysRevB.31.1396.
- [43] A. A. Middleton, Asymptotic uniqueness of the sliding state for charge-density waves, *Phys. Rev. Lett.* **68**(5), 670–673, (1992). doi:10.1103/PhysRevLett.68.670.
- [44] T. Giamarchi, A. Kolton, and A. Rosso. Dynamics of Disordered Elastic Systems. In eds. M. C. Miguel and M. Rubi, *Jamming, Yielding, and Irreversible Deformation in Condensed Matter*, vol. 688, pp. 91–108. Springer-Verlag, Berlin/Heidelberg, (2006). ISBN 978-3-540-30028-1. doi:10.1007/3-540-33204-9_6.
- [45] K. J. Wiese, Theory and experiments for disordered elastic manifolds, depinning, avalanches, and sandpiles, *Reports on Progress in Physics*. **85**(8), 086502, (2022).
- [46] B. Alessandro, C. Beatrice, G. Bertotti, and A. Montorsi, Domain-wall dynamics and Barkhausen effect in metallic ferromagnetic materials. I. Theory, *Journal of Applied Physics*. **68**(6), 2901–2907, (1990). doi:10.1063/1.346423.
- [47] F. Colaiori, Exactly solvable model of avalanches dynamics for Barkhausen crackling noise, *Advances in Physics*. **57**(4), 287–359, (2008). doi:10.1080/00018730802420614.
- [48] P. Le Doussal and K. J. Wiese, Driven particle in a random landscape: Disorder correlator, avalanche distribution, and extreme value statistics of records, *Phys. Rev. E*. **79**(5), 051105, (2009). doi:10.1103/PhysRevE.79.051105.
- [49] P. Le Doussal and K. J. Wiese, Size distributions of shocks and static avalanches from the Functional Renormalization Group, *Phys. Rev. E*. **79**(5), 051106, (2009). doi:10.1103/PhysRevE.79.051106.
- [50] A. Rosso, P. Le Doussal, and K. J. Wiese, Avalanche-size distribution at the depinning transition: A numerical test of the theory, *Phys. Rev. B*. **80**(14), 144204, (2009). doi:10.1103/PhysRevB.80.144204.
- [51] P. Le Doussal and K. J. Wiese, Avalanche dynamics of elastic interfaces, *Physical Review E*. **88**(2), 022106, (2013).
- [52] M. Delorme, P. Le Doussal, and K. Wiese, Distribution of joint local and total size and of extension for avalanches in the Brownian force model, *Phys. Rev. E*. **93**, (2016). doi:10.1103/PhysRevE.93.052142.
- [53] A. Zoia, A. Rosso, and M. Kardar, Fractional laplacian in bounded domains, *Physical Review*

- E.* **76**(2), 021116, (2007).
- [54] J. F. Joanny and P. G. de Gennes, A model for contact angle hysteresis, *The Journal of Chemical Physics*. **81**(1), 552–562, (1984). doi:10.1063/1.447337.
 - [55] H. Gao and J. Rice, A First-Order Perturbation Analysis of Crack Trapping by Arrays of Obstacles, *J. Appl. Mech.-Trans. Asme - J APPL MECH.* **56**, 828–836, (1989). doi: 10.1115/1.3176178.
 - [56] M. J. Alava, P. K. V. V. Nukala, and S. Zapperi, Statistical models of fracture, *Advances in Physics*. **55**(3-4), 349–476, (2006). doi:10.1080/00018730300741518.
 - [57] D. Bonamy, S. Santucci, and L. Ponson, Crackling Dynamics in Material Failure as the Signature of a Self-Organized Dynamic Phase Transition, *Phys. Rev. Lett.* **101**(4), 045501, (2008). doi:10.1103/PhysRevLett.101.045501.
 - [58] P. Le Doussal, K. J. Wiese, E. Raphael, and R. Golestanian, Can Nonlinear Elasticity Explain Contact-Line Roughness at Depinning?, *Phys. Rev. Lett.* **96**(1), 015702, (2006). doi: 10.1103/PhysRevLett.96.015702.
 - [59] D. Bonamy and E. Bouchaud, Failure of heterogeneous materials: A dynamic phase transition?, *Physics Reports*. **498**(1), 1–44, (2011). doi:10.1016/j.physrep.2010.07.006.
 - [60] K. A. Dahmen, Y. Ben-Zion, and J. T. Uhl, Micromechanical model for deformation in solids with universal predictions for stress-strain curves and slip avalanches, *Physical review letters*. **102**(17), 175501, (2009).
 - [61] J. Antonaglia, W. J. Wright, X. Gu, R. R. Byer, T. C. Hufnagel, M. LeBlanc, J. T. Uhl, and K. A. Dahmen, Bulk metallic glasses deform via slip avalanches, *Physical review letters*. **112**(15), 155501, (2014).
 - [62] W. J. Wright, Y. Liu, X. Gu, K. D. Van Ness, S. L. Robare, X. Liu, J. Antonaglia, M. LeBlanc, J. T. Uhl, T. C. Hufnagel, et al., Experimental evidence for both progressive and simultaneous shear during quasistatic compression of a bulk metallic glass, *Journal of Applied Physics*. **119**(8), 084908, (2016).
 - [63] W. J. Wright, A. A. Long, X. Gu, X. Liu, T. C. Hufnagel, and K. A. Dahmen, Slip statistics for a bulk metallic glass composite reflect its ductility, *Journal of Applied Physics*. **124**(18), 185101, (2018).
 - [64] W. H. Herschel and R. Bulkley, Konsistenzmessungen von gummi-benzollösungen, *Kolloid-Zeitschrift*. **39**(4), 291–300 (Aug, 1926). ISSN 1435-1536. doi:10.1007/BF01432034. URL

<https://doi.org/10.1007/BF01432034>.

- [65] G. Ovarlez, L. Tocquer, F. Bertrand, and P. Coussot, Rheopexy and tunable yield stress of carbon black suspensions, *Soft Matter*. **9**(23), 5540–5549, (2013).
- [66] A. Argon, Plastic deformation in metallic glasses, *Acta Metallurgica*. **27**(1), 47 – 58, (1979). ISSN 0001-6160. doi:10.1016/0001-6160(79)90055-5. URL <http://www.sciencedirect.com/science/article/pii/0001616079900555>.
- [67] C. Maloney and A. Lemaitre, Subextensive scaling in the athermal, quasistatic limit of amorphous matter in plastic shear flow, *Phys. Rev. Lett.* **93**, 016001 (Jul, 2004). doi: 10.1103/PhysRevLett.93.016001. URL <http://link.aps.org/doi/10.1103/PhysRevLett.93.016001>.
- [68] K. M. Salerno, C. E. Maloney, and M. O. Robbins, Avalanches in strained amorphous solids: Does inertia destroy critical behavior?, *Phys. Rev. Lett.* **109**, 105703 (Sep, 2012). doi:10.1103/PhysRevLett.109.105703. URL <http://link.aps.org/doi/10.1103/PhysRevLett.109.105703>.
- [69] J. Lin, E. Lerner, A. Rosso, and M. Wyart, Scaling description of the yielding transition in soft amorphous solids at zero temperature, *Proceedings of the National Academy of Sciences*. **111**(40), 14382–14387, (2014).
- [70] J.-C. Baret, D. Vandembroucq, and S. Roux, Extremal model for amorphous media plasticity, *Phys. Rev. Lett.* **89**, 195506 (Oct, 2002). doi:10.1103/PhysRevLett.89.195506. URL <http://link.aps.org/doi/10.1103/PhysRevLett.89.195506>.
- [71] G. Picard, A. Ajdari, F. Lequeux, and L. Bocquet, Elastic consequences of a single plastic event: a step towards the microscopic modelling of the flow of yield stress fluids, *Eur. Phys. Jour. E*. **15**, 371, (2004).
- [72] Z. Budrikis, D. F. Castellanos, S. Sandfeld, M. Zaiser, and S. Zapperi, Universal features of amorphous plasticity, *Nature communications*. **8**(1), 1–10, (2017).
- [73] J. Carlson and J. Langer, Mechanical model of an earthquake fault, *Physical Review A*. **40** (11), 6470, (1989).
- [74] A. Nicolas, E. E. Ferrero, K. Martens, and J.-L. Barrat, Deformation and flow of amorphous solids: Insights from elastoplastic models, *Reviews of Modern Physics*. **90**(4), 045006, (2018).
- [75] X. Cao, A. Nicolas, D. Trimcev, and A. Rosso, Soft modes and strain redistribution in continuous models of amorphous plasticity: The Eshelby paradigm, and beyond?, *Soft Matter*.

- 14**(18), 3640–3651, (2018). doi:10.1039/C7SM02510F.
- [76] M. Muramatsu, T. Irie, and T. Nagatani, Jamming transition in pedestrian counter flow, *Physica A: Statistical Mechanics and its Applications*. **267**(3-4), 487–498, (1999).
 - [77] M. Geiger, L. Petrini, and M. Wyart, Landscape and training regimes in deep learning, *Physics Reports*. **924**, 1–18, (2021).
 - [78] B. Andreotti, Y. Forterre, and O. Pouliquen, *Granular media: between fluid and solid*. (Cambridge University Press, 2013).
 - [79] S. Nowak, A. Samadani, and A. Kudrolli, Maximum angle of stability of a wet granular pile, *Nature Physics*. **1**(1), 50–52, (2005).
 - [80] H. Perrin, C. Clavaud, M. Wyart, B. Metzger, and Y. Forterre, Interparticle friction leads to nonmonotonic flow curves and hysteresis in viscous suspensions, *Physical Review X*. **9**(3), 031027, (2019).
 - [81] J. A. Dijksman, G. H. Wortel, L. T. van Dellen, O. Dauchot, and M. van Hecke, Jamming, yielding, and rheology of weakly vibrated granular media, *Physical review letters*. **107**(10), 108303, (2011).
 - [82] S. Mowlavi and K. Kamrin, Interplay between hysteresis and nonlocality during onset and arrest of flow in granular materials, *Soft Matter*. **17**(31), 7359–7375, (2021).
 - [83] E. DeGiuli and M. Wyart, Friction law and hysteresis in granular materials, *Proceedings of the National Academy of Sciences*. **114**(35), 9284–9289, (2017). URL <http://www.pnas.org/content/114/35/9284.abstract>.
 - [84] O. Pouliquen, Velocity correlations in dense granular flows, *Physical review letters*. **93**(24), 248001, (2004).
 - [85] P. Olsson, Asymmetric velocity correlations in shearing media, *Phys. Rev. E*. **82**(3), 031303 (Sep, 2010). doi:10.1103/PhysRevE.82.031303.
 - [86] G. Düring, E. Lerner, and M. Wyart, Length scales and self-organization in dense suspension flows, *Physical Review E*. **89**(2), 022305, (2014).
 - [87] P. Olsson and S. Teitel, Critical scaling of shearing rheology at the jamming transition of soft-core frictionless disks, *Physical Review E*. **83**(3), 030302, (2011).
 - [88] E. DeGiuli, G. Düring, E. Lerner, and M. Wyart, Unified theory of inertial granular flows and non-Brownian suspensions, *arXiv preprint arXiv:1410.3535*. (2014).
 - [89] H. Perrin, M. Wyart, B. Metzger, and Y. Forterre, Nonlocal effects reflect the jamming

- criticality in frictionless granular flows down inclines, *Physical Review Letters*. **126**, (2021).
- [90] A. J. Liu, S. R. Nagel, W. van Saarloos, and M. Wyart, *The jamming scenario: an introduction and outlook*, In eds. L. Berthier, G. Biroli, J. Bouchaud, L. Cipeletti, and W. van Saarloos, *Dynamical heterogeneities in glasses, colloids, and granular media*, p. 298. Oxford University Press, Oxford, (2010).
 - [91] M. van Hecke, Jamming of soft particles: geometry, mechanics, scaling and isostaticity, *Journal of Physics: Condensed Matter*. **22**(3), 033101–033124, (2010).
 - [92] C. S. O’Hern, L. E. Silbert, A. J. Liu, and S. R. Nagel, Jamming at zero temperature and zero applied stress: The epitome of disorder, *Phys. Rev. E*. **68**(1), 011306–011324 (Jul, 2003). doi:10.1103/PhysRevE.68.011306.
 - [93] P.-E. Peyneau and J.-N. Roux, Frictionless bead packs have macroscopic friction, but no dilatancy, *Physical review E*. **78**(1), 011307, (2008).
 - [94] R. Lespiat, S. Cohen-Addad, and R. Höhler, Jamming and flow of random-close-packed spherical bubbles: An analogy with granular materials, *Phys. Rev. Lett.* **106**, 148302 (Apr, 2011). doi:10.1103/PhysRevLett.106.148302.
 - [95] G. Combe and J.-N. Roux, Strain versus stress in a model granular material: a devil’s staircase, *Physical Review Letters*. **85**(17), 3628, (2000).
 - [96] E. Lerner, G. During, and M. Wyart, Low-energy non-linear excitations in sphere packings, *Soft Matter*. **9**, 8252–8263, (2013). doi:10.1039/C3SM50515D.
 - [97] A. L. Efros and B. I. Shklovskii, Coulomb gap and low temperature conductivity of disordered systems, *Journal of Physics C: Solid State Physics*. **8**(4), L49, (1975). URL <http://stacks.iop.org/0022-3719/8/i=4/a=003>.
 - [98] D. Thouless, P. Anderson, and R. Palmer, Solution of solvable model of a spin glass, *Philo. Mag.* **35**, 593–601 (Jul, 1977). doi:10.1080/14786437708235992. URL <http://link.aps.org/doi/10.1103/PhysRevLett.59.381>.
 - [99] S. Karmakar, E. Lerner, and I. Procaccia, Statistical physics of the yielding transition in amorphous solids, *Phys. Rev. E*. **82**, 055103 (Nov, 2010). doi:10.1103/PhysRevE.82.055103. URL <http://link.aps.org/doi/10.1103/PhysRevE.82.055103>.
 - [100] J. Lin, A. Saade, E. Lerner, A. Rosso, and M. Wyart, On the density of shear transformations in amorphous solids, *EPL (Europhysics Letters)*. **105**(2), 26003, (2014).
 - [101] J. Lin, T. Gueudré, A. Rosso, and M. Wyart, Criticality in the approach to failure in amor-

- phous solids, *Phys. Rev. Lett.* **115**, 168001, (2015).
- [102] M. Müller and M. Wyart, Marginal stability in structural, spin, and electron glasses, *Annual Review of Condensed Matter Physics.* **6**(1), 177–200, (2015). doi:10.1146/annurev-conmatphys-031214-014614.
 - [103] C. E. Maloney and A. Lemaître, Amorphous systems in athermal, quasistatic shear, *Phys. Rev. E.* **74**(1), 016118 (Jul, 2006).
 - [104] C. Kane and T. Lubensky, Topological boundary modes in isostatic lattices, *Nature Physics.* **10**(1), 39–45, (2014).
 - [105] M. Wyart, Marginal stability constrains force and pair distributions at random close packing, *Phys. Rev. Lett.* **109**, 125502 (Sep, 2012). doi:10.1103/PhysRevLett.109.125502.
 - [106] P. Charbonneau, J. Kurchan, G. Parisi, P. Urbani, and F. Zamponi, Fractal free energy landscapes in structural glasses, *Nature Communications.* **5**(3725), (2014).
 - [107] P. Charbonneau, E. I. Corwin, G. Parisi, and F. Zamponi, Jamming criticality revealed by removing localized buckling excitations, *Physical Review Letters.* **114**(12), 125504, (2015).
 - [108] C. P. Goodrich, A. J. Liu, and S. R. Nagel, Finite-size scaling at the jamming transition, *Phys. Rev. Lett.* **109**, 095704 (Aug, 2012). doi:10.1103/PhysRevLett.109.095704. URL <https://link.aps.org/doi/10.1103/PhysRevLett.109.095704>.
 - [109] J. D. Sartor, S. A. Ridout, and E. I. Corwin, Mean-field predictions of scaling prefactors match low-dimensional jammed packings, *Physical Review Letters.* **126**(4), 048001, (2021).
 - [110] F. Behrens, G. Arpino, Y. Kivva, and L. Zdeborová, (dis) assortative partitions on random regular graphs, *arXiv preprint arXiv:2202.10379*. (2022).
 - [111] A. Lemaître and C. Caroli, Plastic response of a two-dimensional amorphous solid to quasistatic shear: Transverse particle diffusion and phenomenology of dissipative events, *Physical Review E.* **76**(3), 036104, (2007).
 - [112] T. Nattermann, Y. Shapir, and I. Vilfan, Interface pinning and dynamics in random systems, *Phys. Rev. B.* **42**(13), 8577–8586, (1990). doi:10.1103/PhysRevB.42.8577.
 - [113] E. Agoritsas, R. García-García, V. Lecomte, L. Truskinovsky, and D. Vandembroucq, Driven interfaces: from flow to creep through model reduction, *Journal of Statistical Physics.* **164**(6), 1394–1428, (2016).
 - [114] A. Tanguy, M. Gounelle, and S. Roux, From individual to collective pinning: Effect of long-range elastic interactions, *Phys. Rev. E.* **58**(2), 1577–1590, (1998). doi:

- 10.1103/PhysRevE.58.1577.
- [115] P. Chauve, T. Giamarchi, and P. Le Doussal, Creep and depinning in disordered media, *Phys. Rev. B.* **62**(10), 6241–6267, (2000). doi:10.1103/PhysRevB.62.6241.
 - [116] X. Cao, S. Bouzat, A. B. Kolton, and A. Rosso, Localization of soft modes at the depinning transition, *Phys. Rev. E.* **97**(2), (2018). doi:10.1103/PhysRevE.97.022118.
 - [117] O. Narayan and D. S. Fisher, Critical behavior of sliding charge-density waves in $4-\epsilon$ dimensions, *Phys. Rev. B.* **46**(18), 11520–11549, (1992). doi:10.1103/PhysRevB.46.11520.
 - [118] T. Nattermann and L.-H. Tang, Kinetic surface roughening. I. The Kardar-Parisi-Zhang equation in the weak-coupling regime, *Phys. Rev. A.* **45**(10), 7156–7161, (1992). doi:10.1103/PhysRevA.45.7156.
 - [119] O. Narayan and D. S. Fisher, Threshold critical dynamics of driven interfaces in random media, *Phys. Rev. B.* **48**(10), 7030–7042, (1993). doi:10.1103/PhysRevB.48.7030.
 - [120] D. Ertas and M. Kardar, Critical dynamics of contact line depinning, *Phys. Rev. E.* **49**(4), R2532–R2535, (1994). doi:10.1103/PhysRevE.49.R2532.
 - [121] P. Chauve, P. Le Doussal, and K. Jörg Wiese, Renormalization of Pinned Elastic Systems: How Does It Work Beyond One Loop?, *Phys. Rev. Lett.* **86**(9), 1785–1788, (2001). doi:10.1103/PhysRevLett.86.1785.
 - [122] P. Le Doussal, K. J. Wiese, and P. Chauve, 2-loop Functional Renormalization Group Theory of the Depinning Transition, *Phys. Rev. B.* **66**(17), (2002). doi:10.1103/PhysRevB.66.174201.
 - [123] P. Le Doussal, K. J. Wiese, and P. Chauve, Functional Renormalization Group and the Field Theory of Disordered Elastic Systems, *Phys. Rev. E.* **69**(2), (2004). doi:10.1103/PhysRevE.69.026112.
 - [124] K. J. Wiese, C. Husemann, and P. Le Doussal, Field theory of disordered elastic interfaces at 3-loop order: The β -function, *Nuclear Physics B.* **932**, 540–588, (2018).
 - [125] C. Husemann and K. J. Wiese, Field theory of disordered elastic interfaces at 3-loop order: Critical exponents and scaling functions, *Nuclear Physics B.* **932**, 589–618, (2018).
 - [126] C. ter Burg, G. Durin, and K. J. Wiese, Force-force correlations in disordered magnets, *arXiv preprint arXiv:2109.01197*. (2021).
 - [127] H. Leschhorn, T. Nattermann, S. Stepanow, and L.-H. Tang, Driven interface depinning in a disordered medium, *Ann. Phys.* **509**(1), 1–34, (1997). doi:10.1002/andp.19975090102.
 - [128] A. Rosso and W. Krauth, Roughness at the depinning threshold for a long-range elastic

- string, *Phys. Rev. E* **65**(2), 025101, (2002). doi:10.1103/PhysRevE.65.025101.
- [129] A. Rosso, A. K. Hartmann, and W. Krauth, Depinning of elastic manifolds, *Phys. Rev. E* **67**(2), 021602, (2003). doi:10.1103/PhysRevE.67.021602.
- [130] O. Duemmer and W. Krauth, Critical exponents of the driven elastic string in a disordered medium, *Phys. Rev. E* **71**(6), (2005). doi:10.1103/PhysRevE.71.061601.
- [131] O. Duemmer and W. Krauth, Depinning exponents of the driven long-range elastic string, *J. Stat. Mech. Theory Exp.* **2007**(01), P01019–P01019, (2007). doi:10.1088/1742-5468/2007/01/P01019.
- [132] E. E. Ferrero, S. Bustingorry, A. B. Kolton, and A. Rosso, Numerical Approaches on Driven Elastic Interfaces in Random Media, *Comptes Rendus Phys.* **14**(8), 641–650, (2013). doi:10.1016/j.crhy.2013.08.002.
- [133] A. Rosso, P. L. Doussal, and K. J. Wiese, Numerical Calculation of the Functional renormalization group fixed-point functions at the depinning transition, *Phys. Rev. B* **75**(22), 220201, (2007). doi:10.1103/PhysRevB.75.220201.
- [134] S. Lemerle, J. Ferré, C. Chappert, V. Mathet, T. Giamarchi, and P. Le Doussal, Domain Wall Creep in an Ising Ultrathin Magnetic Film, *Phys. Rev. Lett.* **80**(4), 849–852, (1998). doi:10.1103/PhysRevLett.80.849.
- [135] N. B. Caballero, E. E. Ferrero, A. B. Kolton, J. Curiale, V. Jeudy, and S. Bustingorry, Magnetic domain wall creep and depinning: A scalar field model approach, *Phys. Rev. E* **97**(6), 062122, (2018). doi:10.1103/PhysRevE.97.062122.
- [136] E. E. Ferrero, L. Foini, T. Giamarchi, A. B. Kolton, and A. Rosso, Creep motion of elastic interfaces driven in a disordered landscape, *ArXiv200111464 Cond-Mat.* (2020).
- [137] L. Laurson, X. Illa, and M. J. Alava, The effect of thresholding on temporal avalanche statistics, *J. Stat. Mech.* **2009**(01), P01019, (2009). doi:10.1088/1742-5468/2009/01/P01019.
- [138] J. Barés, D. Bonamy, and A. Rosso, Seismiclike organization of avalanches in a driven long-range elastic string as a paradigm of brittle cracks, *Phys. Rev. E* **100**(2), 023001, (2019). doi:10.1103/PhysRevE.100.023001.
- [139] C. J. Bolech and A. Rosso, Universal Statistics of the Critical Depinning Force of Elastic Systems in Random Media, *Phys. Rev. Lett.* **93**(12), 125701, (2004). doi:10.1103/PhysRevLett.93.125701.
- [140] V. Démery, A. Rosso, and L. Ponson, From microstructural features to effective toughness

- in disordered brittle solids, *EPL Europhys. Lett.* **105**(3), 34003, (2014). doi:10.1209/0295-5075/105/34003.
- [141] A. A. Fedorenko, P. Le Doussal, and K. J. Wiese, Universal distribution of threshold forces at the depinning transition, *Phys. Rev. E.* **74**(4), 041110, (2006). doi: 10.1103/PhysRevE.74.041110.
 - [142] S. Papanikolaou, F. Bohn, R. L. Sommer, G. Durin, S. Zapperi, and J. P. Sethna, Universality beyond power laws and the average avalanche shape, *Nature Physics.* **7**, 316–320, (2011). doi: 10.1038/NPHYS1884.
 - [143] M. C. Kuntz and J. P. Sethna, Noise in disordered systems: The power spectrum and dynamic exponents in avalanche models, *Physical Review B.* **62**, 11699–11708, (2000).
 - [144] A. P. Mehta, A. C. Mills, K. A. Dahmen, and J. P. Sethna, Universal pulse shape scaling function and exponents: Critical test for avalanche models applied to Barkhausen noise, *Physical Review E.* **65**, 046139, (2002).
 - [145] S. Zapperi, C. Castellano, F. Colaiori, and G. Durin, Signature of effective mass in crackling-noise asymmetry, *Nature Physics.* **1**(1), 46–49, (2005).
 - [146] P. Le Doussal and K. J. Wiese, Distribution of velocities in an avalanche, *EPL (Europhysics Letters).* **97**(4), 46004, (2012).
 - [147] A. Dobrinevski, P. Le Doussal, and K. J. Wiese, Avalanche shape and exponents beyond mean-field theory, *EPL (Europhysics Letters).* **108**(6), 66002, (2015).
 - [148] G. Durin, F. Bohn, M. A. Corrêa, R. L. Sommer, P. Le Doussal, and K. Wiese, Quantitative scaling of magnetic avalanches, *Physical review letters.* **117**(8), 087201, (2016).
 - [149] A. Dobrinevski, P. Le Doussal, and K. J. Wiese, Statistics of avalanches with relaxation and barkhausen noise: A solvable model, *Physical Review E.* **88**(3), 032106, (2013).
 - [150] C. Le Priol, J. Chopin, P. Le Doussal, L. Ponson, and A. Rosso, Universal Scaling of the Velocity Field in Crack Front Propagation, *Phys. Rev. Lett.* **124**(6), 065501, (2020). doi: 10.1103/PhysRevLett.124.065501.
 - [151] K. J. Måløy, S. Santucci, J. Schmittbuhl, and R. Toussaint, Local Waiting Time Fluctuations along a Randomly Pinned Crack Front, *Phys. Rev. Lett.* **96**(4), 045501, (2006). doi: 10.1103/PhysRevLett.96.045501.
 - [152] L. Laurson, S. Santucci, and S. Zapperi, Avalanches and clusters in planar crack front propagation, *Phys. Rev. E.* **81**(4), (2010). doi:10.1103/PhysRevE.81.046116.

- [153] X. Cao, P. L. Doussal, and A. Rosso, Clusters in an epidemic model with long-range dispersal, *arXiv preprint arXiv:2203.14663*. (2022).
- [154] C. Le Priol, P. Le Doussal, and A. Rosso, Spatial clustering of depinning avalanches in presence of long-range interactions, *Physical Review Letters*. **126**(2), 025702, (2021).
- [155] P. Hébraud and F. Lequeux, Mode-coupling theory for the pasty rheology of soft glassy materials, *Phys. Rev. Lett.* **81**, 2934–2937 (Oct, 1998). doi:10.1103/PhysRevLett.81.2934. URL <http://link.aps.org/doi/10.1103/PhysRevLett.81.2934>.
- [156] E. A. Jagla, Avalanche-size distributions in mean-field plastic yielding models, *Physical Review E*. **92**(4), 042135, (2015).
- [157] A. Lemaître and C. Caroli, Plastic response of a 2d amorphous solid to quasi-static shear: li-dynamical noise and avalanches in a mean field model, *arXiv preprint arXiv:0705.3122*. (2007).
- [158] J. Lin and M. Wyart, Mean-field description of plastic flow in amorphous solids, *Physical Review X*. **6**(1), 011005, (2016).
- [159] W. Ji, M. Popović, T. W. de Geus, E. Lerner, and M. Wyart, Theory for the density of interacting quasilocalized modes in amorphous solids, *Physical Review E*. **99**(2), 023003, (2019).
- [160] M. Ozawa, L. Berthier, G. Biroli, A. Rosso, and G. Tarjus, Random critical point separates brittle and ductile yielding transitions in amorphous materials, *Proceedings of the National Academy of Sciences*. **115**(26), 6656–6661, (2018).
- [161] J. Lin and M. Wyart, Microscopic processes controlling the herschel-bulkley exponent, *Physical review E*. **97**(1), 012603, (2018).
- [162] J. T. Parley, R. Mandal, and P. Sollich, Mean-field description of aging linear response in athermal amorphous solids, *Physical Review Materials*. **6**(6), 065601, (2022).
- [163] K. M. Salerno and M. O. Robbins, Effect of inertia on sheared disordered solids: Critical scaling of avalanches in two and three dimensions, *Physical Review E*. **88**(6), 062206, (2013).
- [164] M. Popović, T. W. de Geus, W. Ji, A. Rosso, and M. Wyart, Scaling description of creep flow in amorphous solids, *arXiv preprint arXiv:2111.04061*. (2021).
- [165] N. J. Balmforth, I. A. Frigaard, and G. Ovarlez, Yielding to stress: recent developments in viscoplastic fluid mechanics, *Annu. Rev. Fluid Mech.* **46**(1), 121–146, (2014).
- [166] J. Goyon, A. Colin, and L. Bocquet, How does a soft glassy material flow: finite size effects,

- non local rheology, and flow cooperativity, *Soft Matter*. **6**(12), 2668–2678, (2010).
- [167] T. Gueudré, J. Lin, A. Rosso, and M. Wyart, Scaling description of non-local rheology, *Soft Matter*. **13**(20), 3794–3801, (2017).
- [168] M. Popović, T. W. de Geus, W. Ji, and M. Wyart, Thermally activated flow in models of amorphous solids, *Physical Review E*. **104**(2), 025010, (2021).
- [169] E. E. Ferrero, A. B. Kolton, and E. A. Jagla, Yielding of amorphous solids at finite temperatures, *Physical Review Materials*. **5**(11), 115602, (2021).
- [170] P. Le Doussal, M. Müller, and K. J. Wiese, Equilibrium avalanches in spin glasses, *Phys. Rev. B*. **85**, 214402 (Jun, 2012). doi:10.1103/PhysRevB.85.214402. URL <http://link.aps.org/doi/10.1103/PhysRevB.85.214402>.
- [171] S. Franz and S. Spigler, Mean-field avalanches in jammed spheres, *Physical Review E*. **95**(2), 022139, (2017).
- [172] I. Balog, G. Tarjus, and M. Tissier, Dimensional reduction breakdown and correction to scaling in the random-field Ising model, *Phys. Rev. E*. **102**, 062154 (Dec, 2020). doi:10.1103/PhysRevE.102.062154. URL <https://link.aps.org/doi/10.1103/PhysRevE.102.062154>.
- [173] L. X. Hayden, A. Raju, and J. P. Sethna, Unusual scaling for two-dimensional avalanches: Curing the facetting and scaling in the lower critical dimension, *Phys. Rev. Research*. **1**, 033060 (Oct, 2019). doi:10.1103/PhysRevResearch.1.033060. URL <https://link.aps.org/doi/10.1103/PhysRevResearch.1.033060>.
- [174] M. Shimada, H. Mizuno, M. Wyart, and A. Ikeda, Spatial structure of quasilocalized vibrations in nearly jammed amorphous solids, *Physical Review E*. **98**(6), 060901, (2018).
- [175] P. Olsson and S. Teitel, Critical Scaling of Shear Viscosity at the Jamming Transition, *Phys. Rev. Lett.* **99**, 178001, (2007).
- [176] C. Heussinger and J.-L. Barrat, Jamming transition as probed by quasistatic shear flow, *Phys. Rev. Lett.* **102**, 218303, (2009).
- [177] E. Lerner, E. DeGiuli, G. Düring, and M. Wyart, Breakdown of continuum elasticity in amorphous solids, *Soft Matter*. **10**, 5085–5092, (2014).
- [178] P. Olsson, Dimensionality and viscosity exponent in shear-driven jamming, *Physical Review Letters*. **122**(10), 108003, (2019).
- [179] M. Trulsson, B. Andreotti, and P. Claudin, Transition from the viscous to inertial regime in

- dense suspensions, *Physical review letters*. **109**(11), 118305, (2012).
- [180] E. DeGiuli, G. Düring, E. Lerner, and M. Wyart, Unified theory of inertial granular flows and non-brownian suspensions, *Physical Review E*. **91**(6), 062206 (06, 2015).
 - [181] R. Mari, R. Seto, J. F. Morris, and M. M. Denn, Shear thickening, frictionless and frictional rheologies in non-brownian suspensions, *Journal of Rheology (1978-present)*. **58**(6), 1693–1724, (2014).
 - [182] M. Wyart and M. Cates, Discontinuous shear thickening without inertia in dense non-brownian suspensions, *Physical review letters*. **112**(9), 098302, (2014).
 - [183] C. Clavaud, A. Bérut, B. Metzger, and Y. Forterre, Revealing the frictional transition in shear-thickening suspensions, *Proceedings of the National Academy of Sciences*. **114**(20), 5147–5152, (2017).
 - [184] J. Comtet, G. Chatté, A. Niguès, L. Bocquet, A. Siria, and A. Colin, Pairwise frictional profile between particles determines discontinuous shear thickening transition in non-colloidal suspensions, *Nature communications*. **8**(1), 1–7, (2017).
 - [185] M. Ramaswamy, I. Griniasty, D. B. Liarte, A. Shetty, E. Katifori, E. D. Gado, J. P. Sethna, B. Chakraborty, and I. Cohen. Universal scaling of shear thickening transitions. <https://arxiv.org/abs/2107.13338>, (2021).
 - [186] M. Ramaswamy, I. Griniasty, J. P. Sethna, B. Chakraborty, and I. Cohen, Incorporating tunability into a universal scaling framework for shear thickening, *arXiv e-prints*. art. arXiv:2205.02184 (May, 2022).
 - [187] M. Trulsson, E. DeGiuli, and M. Wyart, Effect of friction on dense suspension flows of hard particles, *arXiv preprint arXiv:1606.07650*. (2016).
 - [188] M. Ramaswamy, I. Griniasty, D. B. Liarte, A. Shetty, E. Katifori, E. Del Gado, J. P. Sethna, B. Chakraborty, and I. Cohen, Universal scaling of shear thickening transitions, *arXiv preprint arXiv:2107.13338*. (2021).
 - [189] E. DeGiuli and M. Wyart, Unifying suspension and granular flows near jamming, *EPJ Web Conf*. **140**, 01003, (2017). URL <https://doi.org/10.1051/epjconf/201714001003>.
 - [190] G. Zheng and J. R. Rice, Conditions under which velocity-weakening friction allows a self-healing versus a cracklike mode of rupture, *Bulletin of the Seismological Society of America*. **88**(6), 1466–1483, (1998).
 - [191] J. Schwarz and D. Fisher, Depinning with Dynamic Stress Overshoots: Mean Field Theory,

- Phys. Rev. Lett.* **87**(9), 096107, (2001). doi:10.1103/PhysRevLett.87.096107.
- [192] A. Nicolas, J.-L. Barrat, and J. Rottler, Effects of inertia on the steady-shear rheology of disordered solids, *Physical review letters*. **116**(5), 058303, (2016).
 - [193] T. W. de Geus and M. Wyart, Scaling theory for the statistics of slip at frictional interfaces, *arXiv preprint arXiv:2204.02795*. (2022).
 - [194] M. Ozawa, L. Berthier, G. Biroli, and G. Tarjus, Rare events and disorder control the brittle yielding of amorphous solids, *arXiv preprint arXiv:2102.05846*. (2021).
 - [195] M. Popović, T. W. J. de Geus, and M. Wyart, Elastoplastic description of sudden failure in athermal amorphous materials during quasistatic loading, *Physical Review E*. **98**(4) (Oct, 2018). ISSN 2470-0045, 2470-0053. doi:10.1103/PhysRevE.98.040901. URL <https://link.aps.org/doi/10.1103/PhysRevE.98.040901>.
 - [196] S. M. Fielding. Yielding, shear banding and brittle failure of amorphous materials, (2021).
 - [197] D. Richard, C. Rainone, and E. Lerner, Finite-size study of the athermal quasistatic yielding transition in structural glasses, *The Journal of Chemical Physics*. **155**(5), 056101, (2021).
 - [198] R. N. Chacko, F. P. Landes, G. Biroli, O. Dauchot, A. J. Liu, and D. R. Reichman, Elastoplasticity mediates dynamical heterogeneity below the mode coupling temperature, *Physical Review Letters*. **127**(4), 048002, (2021).